Bioorganic & Medicinal Chemistry 24 (2016) 53–72

Contents lists available at ScienceDirect

Bioorganic & Medicinal Chemistry

journal homepage: www.elsevier.com/locate/bmc

Chlorophenoxy aminoalkyl derivatives as histamine H_3R ligands and antiseizure agents

Kamil Kuder [a,†], Dorota Łażewska [a,†], Gniewomir Latacz [a], Johannes Stephan Schwed [b], Tadeusz Karcz [a], Holger Stark [b], Janina Karolak-Wojciechowska [c], Katarzyna Kieć-Kononowicz [a,*]

[a] Jagiellonian University Medical College, Faculty of Pharmacy, Department of Technology and Biotechnology of Drugs, Medyczna 9, 30-688 Kraków, Poland
[b] Institute of Pharmaceutical and Medicinal Chemistry, Heinrich-Heine-University, Universitaetsstr. 1, 40225 Duesseldorf, Germany
[c] Institute of General and Ecological Chemistry, Technical University of Łódź, Żeromskiego 116 Str., 90-924 Łódź, Poland

ARTICLE INFO

Article history:
Received 12 August 2015
Revised 12 November 2015
Accepted 19 November 2015
Available online 2 December 2015

Keywords:
Histamine H_3 receptor
Histamine H_3R ligands
Anticonvulsant
Ethers
Piperidine derivatives
Drug-like properties

ABSTRACT

A series of twenty new chlorophenoxyalkylamine derivatives (**9**–**28**) was synthesized and evaluated on their binding properties at the human histamine H_3 receptor (hH_3R). The spacer alkyl chain contained five to seven carbon atoms. The highest affinities have shown the 4-chloro substituted derivatives **10** and **25** (K_i = 133 and 128 nM, respectively) classified as antagonists in cAMP accumulation assay (EC_{50} = 72 and 75 nM, respectively). Synthesized compounds were also evaluated for anticonvulsant activity in Antiepileptic Screening Program (ASP) at National Institute of Neurological Disorders and Stroke (USA). Two compounds (4-chloro substituted derivatives: **20** and **26**) were the most promising and showed in the MES seizure model in rats (after ip administration) ED_{50} values of 14 mg/kg and 13.18 mg/kg, respectively. Protective indexes (PI = TD_{50}/ED_{50}) were 3.2 for **20** and 3.8 for **26**. Moreover, molecular modeling and docking studies were undertaken to explain affinity at hH_3R of target compounds, and the experimentally and in silico estimation of properties like lipophilicity and metabolism was performed. Antiproliferative effects have been also investigated in vitro for selected compounds (**10** and **25**). These compounds neither possessed significant antiproliferative and antitumor activity, nor modulated CYP3A4 activity up to concentration of 10 μM.

1. Introduction

Histamine receptors belong to the class A super family of G-protein coupled receptors (GPCR).[1] Histamine H_3 receptors (H_3R) are involved in the central and peripheral regulation of histamine levels[2,3] as well as other neurotransmitters such as acetylcholine (Ach), serotonin (5-HT), noradrenalin (NA), and neuropeptide Y, by postsynaptic modulation.[4,5] Therefore, the blockade of these receptors by inhibiting post synaptic H_3R might be a useful pharmacological target in the treatment of many CNS-based diseases. Intensive pharmacological studies suggested the utility of histamine H_3R antagonists/inverse agonists in treatment of various diseases: schizophrenia, Alzheimer (AD) and Parkinson's disease, obesity, narcolepsy and attention-deficit hyperactivity disorder (ADHD),[6–8] also as dual acting ligands with additionally different pharmacological activity.[9–12] Epilepsy could be another indication as experimental findings showed the effectiveness of histamine H_3R antagonists/inverse agonists in various experimental models of epilepsy.[13] Epilepsy, as one of the major neurological disorders, is characterized by unprovoked or reflex seizures.[14] The mechanism of seizures is still not fully understood[15] and available antiepileptic drugs (AEDs) could not help all epileptic patients as almost 30% of them are resistant to current therapy. Moreover, as long life medication is required, caused side effects should be minimized, and the search for new and more efficacious AEDs with good safety profile is important. Conducted research studies show an association between histaminergic central nervous system and seizure pathophysiology. Histamine itself is considered as an endogenous anticonvulsant,[16] whereas histamine H_1 receptor antagonists induce convulsions.[17,18] Recent studies in a lamotrigine-resistant kindled model of epilepsy in mice showed decreased level of brain histamine and suggested a role of this neurotransmitter in resistance development.[19] Last two years have brought more information of anticonvulsant activities of histamine H_3R antagonists/inverse agonists tested in animal models of epilepsy.[20,21] Both imidazole[20] as well as nonimidazole histamine H_3R[21] ligands

* Corresponding author. Tel.: +48 12 6205580.
E-mail address: mfkonono@cyf-kr.edu.pl (K. Kieć-Kononowicz).
† These authors contributed equally to this manuscript.

http://dx.doi.org/10.1016/j.bmc.2015.11.021
0968-0896/

showed some kind of protection in the maximal electroshock (MES)-induced seizure in Wistar rats. Activity mostly depended on the chemical structure of tested compounds. Hybrid molecules,[21] combining H_3R pharmacophore motif (3-piperidopropyloxy moiety) with main structural elements of known AEDs (e.g., the hydantoin element of phenytoin; PHT), unfortunately did not lead to high protection against seizures induced in rats by MES or pentylenetetrazole (PTZ)-kindled epilepsy (up to a dose of 10 mg/kg ip of tested compounds). One PHT derivative showed only moderate protection whereas the another one even induced epileptogenic effect.[21] In mice model of temporal lobe epilepsy (TLE), where seizures are induced by injection of kainic acid (KA), the known histamine H_3R ligand—ABT-239 (3 mg/kg ip) significantly attenuated seizures elicited by KA.[22] This research showed also that coadministration of ABT-239 with sodium valproate (150 mg/kg ip) enhanced anticonvulsive effect. Moreover, this study confirmed the neuroprotective ability of ABT-239 observed previously in mice model of Alzheimer disease.[23]

Amongst a number of active compounds obtained in both academia and industry, so far only one histamine H_3R antagonist, *pitolisant* (PIT; Bioprojet Biotech; Fig. 1) completed phase III of clinical trials with positive results in narcolepsy and daytime sleepiness in Parkinson's disease,[14,24,25] and is under evaluation as an orphan drug (Wakix; *pitolisant* hydrochloride) by Bioprojet Pharma.[26] Recently, clinical utility of PIT was also checked in early phase II studies in the human photosensitivity model.[27] PIT tested in doses of 20, 40 and 60 mg/kg caused statistically significant suppressive effect in 64% of patients.

Since years our research group is engaged in the search for potent histamine H_3R compounds.[28–31] Some time ago we obtained and described a series of diether histamine H_3R ligands, that showed very good histamine H_3R affinities (hH_3R K_i = 3.2–62 nM; selected compounds **1**–**3** are shown in Fig. 1).[30,31]

Encouraged by the aforementioned results in experimental and clinical studies we decided to test selected of our compounds in MES-induced and PTZ-kindled seizure models in rats.[32] A few of these compounds showed promising anticonvulsant activity, among which was compound **1** (Fig. 1). In the MES-induced seizure **1** (10 mg/kg ip; rats) showed protective effects significantly greater than those of PIT. Moreover, derivative **1** (5 mg/kg ip; rats; the lowest effective dose) concomitant with PHT (5 mg/kg ip; rats; ineffective dose) reduced the duration of tonic hind limb extension. Taking into account these results we decided to obtain *N*-alkyl (substituted)(homo)piperidine ether derivatives. As a lead structures for the introduced modifications, a drug candidate *pitolisant* (Wakix®) and compound **1** have been chosen. Modifications included: introduction only one ether group, placing ether group straightaway to the phenyl ring, different cycloalkylamine moieties in the basic part of compounds, ascending alkyl chain length (5–7 methylene groups) as well as changeable position of chlorine in the benzene ring (3-Cl or 4-Cl). General structures of final compounds **9**–**28** are presented in Scheme 1. Compound **9** was preliminary tested in the-MES-induced and PTZ-kindled seizure models in rats at a dose of 10 mg/kg (ip) as described by Sadek et al.[32] The results showed some kind of anticonvulsant protection[32] but lower than for **1**. Considering the above, we examined the whole series of compounds (**9**–**28**) for their anticonvulsant activity and neurotoxicity within the Anticonvulsant Screening Program (ASP) carried out at National Institute of Neurological Disorders and Stroke, National Institutes of Health (Rockville, USA). In vitro pharmacological evaluation of compounds (**9**–**28**) included histamine hH_3R affinity in a binding assay (HEK 239 cells) and in cAMP accumulation assay at HEK293 cells. Moreover, as absorption, distribution, metabolism, elimination and toxicity (ADME-Tox) are very important properties of compounds, in vitro studies are often applied at the earlier stages of drug discovery. We have chosen two the most potent compounds and evaluated their antiproliferative effects and metabolic stability. Lipophilicity using planar RP-TLC method and molecular modelling studies were also included for better understanding behaviour and properties of the compounds.

2. Results and discussion

2.1. Chemistry

The synthesis of desired ether derivatives **9**–**28** was achieved through the efficient synthetic route outlined in Scheme 1.

Chlorophenoxyalkyl bromides (**4**–**8**) were obtained in simple one-step alkylation of suitable chlorophenols with α,ω-dibromoalkanes refluxed in sodium propanolate. Obtained bromides were then reacted with corresponding piperidines and a homopiperidine in the mixture of ethanol/water with powdered potassium carbonate and a catalytic amount of potassium iodide. 3-Methylpiperidine was used as a racemic mixture. The desired products were obtained as free bases and crystallized as salt of oxalic acid. The structures of compounds were confirmed by elemental and spectral analyses (^{1}H NMR, ^{13}C NMR, MS, UV, IR). All compounds except **9** are new ones.[33,34] Compound **9** (free base) was prepared some time ago (1958) as analgesic agent but proved only weak activity.[33]

2.2. Pharmacology

2.2.1. Histamine H_3 receptor affinity

All compounds in their hydrogen oxalate forms were evaluated in radioligand displacement binding assays for affinity at human recombinant histamine H_3 receptor (hH_3R) stably expressed in human embryonic kidney (HEK-239) cells as described by Kottke et al.[35] The radioligand [^{3}H]N^α methylhistamine was used as competitor.

Pharmacological results are assembled in the Table 1. All of the compounds, except compound **24** (due to its very low solubility) showed moderate affinities for hH_3R in nanomolar concentration range (K_i: 128–805 nM). Moreover, most of the compounds showed affinities in K_i range of 100–500 nM (with exception of compounds **11**, **23** and **24**).

For the tested group of novel ligands, amongst four different used cycloalkylamine moieties (piperidine, 3-methylpiperidine, 4-methylpiperidine, homopiperidine), it could be clearly seen, that 3-methylpiperidine is the most preferable basic moiety for histamine H_3R binding pocket. Surprisingly, in the group of heptyl derivatives (e.g., compounds **22** and **26**) 3-methylpiperidine showed slightly lower affinity in comparison to 'bare' piperidine derivatives (e.g., **21** vs **22**; hH_3R K_i = 333 ± 45 vs K_i = 466 ± 146 nM, respectively). On the other hand, for 3-Cl series of compounds, elongation of the alkyl chain resulted in the decrement of histamine H_3R affinity (**14** vs **22**—hH_3R K_i = 174 ± 46 vs K_i = 446 ± 146 nM, respectively), whereas in 4-Cl series elongation of the alkyl spacer resulted in high increment of the affinity (e.g., **9** vs **17** vs **25**; hH_3R K_i = 427 ± 83 vs K_i = 265 ± 128 vs K_i = 128 ± 49 nM, respectively). Compound **25** showed in fact the highest affinity towards hH_3R in the tested group of compounds. However, compound **17**, being direct structural homologue of *pitolisant*, showed radical loss of affinity when compared to the reference ligand (hH_3R K_i = 265 ± 128 nM vs K_i = 0.3—1 nM,[24] respectively). This situation clearly shows that the position of ether moiety plays a crucial role in receptor–ligand interactions for this group of derivatives. Also, the exchange of the one ether moiety in compound **1** for methylene group as in compound **25** had not positive impact on histamine H_3R affinity (hH_3R K_i = 3.20 nM[30] for **1** vs K_i = 128 ± 49 nM for **25**). In summary, compounds with chloro

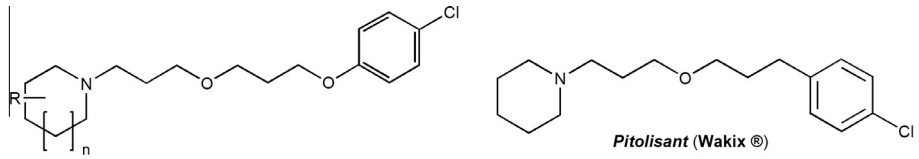

1: n = 1, R = 3-CH_3 hH_3R K_i: 3.20 nM
2: n = 1, R = 4-CH_3 hH_3R K_i: 27.93 nM
3: n = 2, R = H hH_3R K_i: 3.48 nM

hH_3R K_i: 0.3 - 1 nM
rH_3R K_i: 17 nM
ED_{50} = 1.5 mg/kg

Figure 1. In vitro activity of selected previously described H_3R ligands.[30] In vitro and in vivo activity of *pitolisant* (Wakix®).[24]

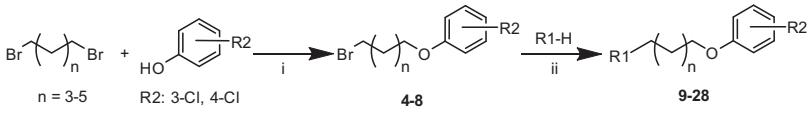

n = 3-5 R2: 3-Cl, 4-Cl **4-8** **9-28**

Compounds							
R1	n	R2		R1	n	R2	
		4-Cl	3-Cl			4-Cl	3-Cl
	3	**9**	---		3	**11**	---
	4	**17**	**13**		4	**19**	**15**
	5	**25**	**21**		5	**27**	**23**
	3	**10**	---		3	**12**	---
	4	**18**	**14**		4	**20**	**16**
	5	**26**	**22**		5	**28**	**24**

Scheme 1. Synthetic pathway of described compounds **9**–**28**. Reagents and conditions: (i) sodium propanolate (0.05 mol Na in 50 mL), room temperature, 15′; 60 °C 3 h; reflux 3 h; 32–74% (ii) K_2CO_3, KI, EtOH, H_2O, reflux 20 h, 17–62%.

substituent in the *para*-position of the phenyl ring seem to confer higher affinities than those of *meta*-substituted (being seven of them **10**, **18**, **19**, **20**, **25**, **26** and **28** with hH_3R K_i < 250 nM). It can be then concluded, that chloro substitution in the 4-position of phenyl moiety is the most favorable for the binding pocket of histamine H_3R among the examples in this small series.

2.2.2. Functional properties at histamine H_3 receptor

Selected structures (**10** and **25**) were additionally tested in cAMP accumulation assay at HEK293 cells expressing recombinant hH_3R. Addition of considered compounds resulted in a blockade of histamine H_3R agonist activity, leading to dose-dependent increase of cAMP level in cells co-treated with H_3R agonist ((*R*)(−)-α-methylhistamine) and forskolin (H_3R is a G_i-coupled receptor). Basing on the obtained results **10** and **25** were classified as histamine H_3R antagonists. Antagonist potencies (EC_{50}) determined in functional assays were as follows: **10**—EC_{50} = 72 ± 8 nM; **25**—EC_{50} = 75 ± 17 nM (Fig. 2).

2.2.3. Anticonvulsant activity

Antiepileptic tests were carried out at National Institute of Neurological Disorders and Stroke, National Institutes of Health (Rockville, USA) within Anticonvulsant Screening Program (ASP) according to known procedures.[36,37] In vivo screening tests in mice included: the maximal electroshock (MES), subcutaneous pentetrazole (scMET) and neurotoxicity test (TOX, rotarod). In the MES and scMET tests activity against generalized tonic–clonic seizures and nonconvulsive (absence or myoclonic) seizures might be predicted, respectively.[38]

Results of the anticonvulsant screening are presented in Table 2. In the scMET test none of the tested compounds showed any protection. In the MES test compounds were administered in mice intraperitoneally (ip) in the doses from 3 to 300 mg/kg, mostly in the dose of 30 mg/kg. All of them (except **21**–**24**) showed some kind of protection at this dose (30 mg/kg) at 30 min after administration. A few compounds which were active at the dose of 100 mg/kg (**13**–**15**, **18**, and **22**–**28**) showed also protection at the both tested times (30 min and 4 h). In the rotarod test compounds revealed toxicity especially in the higher doses (100 mg/kg and 300 mg/kg). In the most cases they caused inability to grasp rotarod or/and death.

Two compounds **20** and **26** were also tested in the MES test in rats after ip administration. Data are collected in Table 3. Both of them were active but compound **26** showed 100% protection lasting from 0.5 h to 4 h.

According to ASP procedures for most promising compounds in the MES test in mice (**9**, **10**, **13**–**15**, **18**–**20**, and **25**–**28**; Table 2) showing anticonvulsant activity at the dose of 30 mg/kg and no neurotoxicity at the same dose, additional MES tests in rats after oral administration were performed. Results are presented in Table 4 (Supplemental materials). Only three compounds (**9**, **14** and **27**) were devoid of anticonvulsant protection, whereas the other showed some kind of activity protecting in most cases 25% of animals in two time points. All compounds in the tested dose 30 mg/kg did not show any toxicity.

Selected compounds were screened to block psychomotor seizures induced by low-frequency (6 Hz) and longer duration of stimuli (3 s) delivered through corneal electrodes (test 6 Hz; Table 5). Compounds effective in the 6 Hz test can be useful in the treatment of pharmacoresistant epilepsy.[38] Only two compounds **15** and **26** showed some protection (from 25% to 100%) in all the tested time at the dose 50 mg/kg and 60 mg/kg respectively. Three compounds (**17**, **19** and **26**) were tested at two doses, but no protection was observed at the lowest one. All compounds showed high toxicity in the active dose. For compound **20** even TOX ED_{50} value was calculated: TOX ED_{50} = 36.2 mg/kg (t = 0.25 h).

Four the most promising compounds (**18**, **19**, **20** and **26**) were selected for quantitative evaluation in mice or/and rats via ip administration. The tests provided an evaluation of the ED_{50} and TD_{50} values and the data are shown in Table 6. The ED_{50} values are from 13.04 mg/kg for **19** (mice) to 16.80 mg/kg for **18** (mice). Calculated protection index PI (PI = TD_{50}/ED_{50}) values for **18**, **19**,

Table 1
Human histamine H_3 receptor in vitro affinities of compounds **9**–**28**

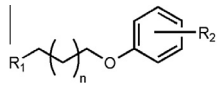

No.	R1	*n*	R2	hH_3R[a] K_i (nM)
9		3	4-Cl	427 ± 83[b]
10		3	4-Cl	133 ± 39
11		3	4-Cl	800 ± 237
12		3	4-Cl	371 ± 91
13		4	3-Cl	255 ± 10
14		4	3-Cl	174 ± 46
15		4	3-Cl	412 ± 10
16		4	3-Cl	293 ± 78
17		4	4-Cl	265 ± 128
18		4	4-Cl	205 ± 49
19		4	4-Cl	189 ± 110
20		4	4-Cl	237 ± 138
21		5	3-Cl	333 ± 35
22		5	3-Cl	466 ± 146
23		5	3-Cl	805 ± 2
24		5	3-Cl	>150,000[c]
25		5	4-Cl	128 ± 49
26		5	4-Cl	180 ± 75
27		5	4-Cl	467 ± 41
28		5	4-Cl	203 ± 48

[a] [^{3}H]N^{α}-methylhistamine binding assay performed with cell membrane preparation of HEK-hH_3R cells stably expressing human H_3 receptor, mean value ± SEM, $n = 3$; measurement as previously described.[35]
[b] Ref. 32.
[c] Difficulties with solubility.

20 and **26** are about 3 (PI: 3 for **18** and **26** in mice; 3.1 for **19** in mice, and PI: 3.2 for **20** and 3.8 for **26** in rats) and are comparable to PI values for phenobarbital (ED_{50} = 21.8 mg/kg, TD_{50} = 69.0 mg/kg; PI = 3.2; data from Ref. 36) and lamotrigine (ED_{50} = 7.47 mg/kg, TD_{50} = 30 mg/kg; PI = 4.0; data from Ref. 36). PI values ~3 are not high and suggest that the tested compounds (**18**, **19**, **20** and **26**) can exert antiepileptic effects but with minor motor disturbances.

Six compounds (**17**–**21** and **26**) were assessed for their ability to halt pilocarpine-induced convulsive status epilepticus in rats (ip).[38] Tested compounds (**17**–**21**) at a dose 65 mg/kg and **26** at a dose 50 mg/kg did not show any protection but some animals died during the testing (Table 7; Supplemental materials). Compound **20** was also tested in a mouse model of temporal lobe epilepsy (the corneal kindled mouse model).[38,39] However, in the dose of 30 mg/kg **20** did not show any protection.

Selected compounds (**17**, **18**, **19**, **20**) were also tested in neuroprotection studies. Severe and repetitive seizures (e.g., status epilepticus) could lead to neuronal damage and death.[40] Tested compounds did not show any cytoprotection against cells death caused by either KA (kainic acid) or NMDA (*N*-methyl-D-aspartate).

As certain antiepileptic drugs possess analgesic activity[41] (e.g., carbamazepine, lamotrigine), therefore, many drug candidates for epilepsy, still in preclinical stage, are evaluated for their analgesic potency. The formalin test is usually performed to study whether the compound possesses any analgesic activity.[42] Compounds **19** (13 mg/kg; 0.25 h) and **26** (16 mg/kg; 0.25 h) did not cause scientifically significant decrease of animals' pain response in either acute and inflammatory phase.

Analyzing the anticonvulsant activities of the synthesized compounds it was noticeable that most compounds showing anticonvulsant activity contain chloro substituent in the *para* position of the benzene ring. Moreover, more active were compounds with a chain of six carbon atoms as more of them reached to further ASP phases. However, in the whole series of compounds, **20** (hexyl derivative) and **26** (heptyl derivative) are considered as the most active. Unfortunately no straight correlation between hH_3R affinity and anticonvulsant activity of compounds can be seen. The most active in ASP compounds **20** and **26** are not the most potent hH_3R ligands (K_i values about 200 nM vs K_i values about 130 nM for **10** and **25**; Table 1). Discrepancies could be connected with species differences in affinities.[43] In vivo tests were conducted in rodents whereas in vitro binding assay on HEK-293 cell stably expressing hH_3R.

2.3. X-ray studies and in silico molecular and docking studies

Monocrystal of compound **19** (in the hydrogen oxalate form) was selected as suitable for X-ray structure analysis. Molecule adopts extended conformation and proton is located at *N1* nitrogen. In the structure hydrogen oxalate ion was also located (charge on O2B atom). Both charged species are joined via three H-bonds: N1–H1...O2B = 2.843(4) Å, N1–H1...O1B = 2.932(4) Å and O1A–H1A...O2B = 2.522(3) Å. Finally in the crystal protonated main species are fastened to oxalate ions chain (for details see Fig. 3).

Computational approaches using Schrödinger Maestro 9.3.5[44] allowed the in silico visualization of the investigated compounds binding to histamine H_3R model obtained from GPCRM Structure Modeling Server.[45] The model was built on the crystal structure of M_3 muscarinic acetylcholine receptor, due to its' highest sequence homology to histamine H_3R aa sequence (PDB code: 4DAJ; resolution: 3.4 Å). Validation with reference ligand *pitolisant* according to the procedure described by Levoin et al. was also performed.[45] Docking studies results were interpreted by the values of Docking Score function that resulted in the range of −7.95 to −4.12. Previously described salt bridge formation between the protonated cycloalkylamine nitrogen and GLU206[31] could be observed for most of the compounds despite their in vitro activity. As it has been previously stated, this might be a crucial residue for antagonists binding at the histamine H_3R.[45,46] Moreover, for all of the ligands π–π stacking could be observed between TYR189 and chlorinated phenyl ring. Interestingly for methylated piperidine derivatives which have higher in vitro affinity than

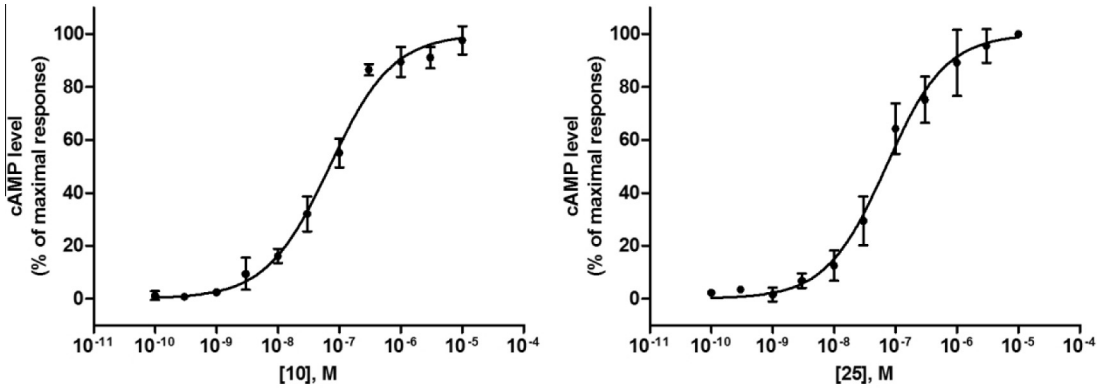

Figure 2. cAMP accumulation studies in HEK293 cells expressing the hH_3R, co-treated with forskolin, (*R*)(−)-α-methylhistamine and tested compounds: **10** (left) and **25** (right).

non-methylated ones, nonadditional interactions between the methyl group and side-chains amino acids were found. A binding modes of compounds **10** and **19** with histamine H_3R homology model are presented in Figure 4. In order to test the possible influence of methyl group and its position on ligands affinity, possible Van der Waal's interactions between the ligand and binding site aminoacids in the distance of 12 Å from ligand were studied. It appeared that the interaction strength were higher for 3-methyl derivatives than for 4-methyl derivatives (e.g., THR375 **10** vs **11**: −1.4 vs −0.94), as well as methylated versus non-methylated piperidine derivatives.

For all of the docked ligands after superimposition it could be observed, that regardless of the alkyl chain length chloro substituted phenyl rings are situated in close proximity of TRP 174, LEU 177, ALA 190, GLU 191, TYR 194, TRP 196. The reason for this is probably the result of the interaction between lipophilic part of the ligands and the functional groups of five partly polar and partly lipophilic amino acids constituting the pocket at receptor binding site.

2.4. Lipophilicity evaluation by RP-TLC

As there is a strong aim to determine physicochemical properties of novel compounds at the early stage of preclinical research, their lipophilicity was experimentally evaluated (expressed by R_{M0} values) using planar RP-TLC method.[47] As a mobile phase, ternary solvent mixture—methanol/acetic acid/water—was used, with constant, 10% acetic acid concentration and varying methanol concentration in the range of 50–80%. Tested set of compounds showed R_{M0} values in the range between 0.914 and 1.505. Lipophilicity studies data are collected in Table 8.

As it was assumed, lipophilicity rises with the elongation of the alkyl chain. Moreover, for structural analogues (3-Cl and 4-Cl derivatives) values resulted in the similar range, for example, compounds **13**–**16** and **17**–**20**. Similar dependence could be observed for 3- and 4-methylpiperidine structural isomers, for example, compounds **10** and **11**. Slightly lower values could be observed for homopiperidine derivatives in comparison with 3 (4)-methylpiperidine analogues. No correlation between lipophilicity and hH_3R affinity was observed for the tested series (data not shown) as well as for lipophilicity and anticonvulsant activity.

In order to compare the theoretical partition coefficient parameters (*clogP*) with practical ones, calculations using computer various programs: Chem3D, Marvin and QikProp for Schrödinger were also performed.[44,48,49] All of the compounds were used in ionic forms. Such obtained theoretical values seem to be more realistic, bearing in mind that all of the tested compounds are hydrogen oxalates. Most similar theoretical-to-practical values were obtained using Marvin software ($R = 0.91598$, $R^2 = 0.83902$, SD = 0.38036).

2.5. Antiproliferative effect study

The most active H_3R ligands described in this study **10** and **25** were chosen to examine the selected ADME-TOX parameters—toxicity and metabolic stability. The drug candidates which have acceptable ADME-TOX parameters are defined as a drug-like and are suitable to the human Phase I clinical trials.[50] The formazan dye based EZ4U was applied for determination of the effect of both tested compounds on proliferation of two eukaryotic cell lines—human embryonic kidney HEK-293 cell line and neuroblastoma IMR-32 cell line. The results were next compared to the reference compound doxorubicin (DX). As was shown below, the incubation of HEK-293 cells in the different concentrations of H_3R ligands for 48 h revealed the dose dependent antiproliferative effect (Fig. 5). The significant inhibition of cell viability was observed above 10 μM for **25** whereas for **10** at only 250 μM. However comparing the IC_{50} values of the reference compound DX ($IC_{50} = 0.46$ μM) with the calculated IC_{50} value for **25** ($IC_{50} = 33.62$ μM), the similar effect of H_3R ligand **25** was observed at more than 70-fold higher concentration.

The observed antiproliferative effect of the examined compounds against neuroblastoma cell line IMR-32 was slightly higher than against HEK-293 (Fig. 6). The calculated IC_{50} values were 15.5 μM for **25** and 89.0 μM for **10**. However, relative to the calculated DX IC_{50} value ($IC_{50} = 0.0051$ μM) the examined compounds did not possess significant antiproliferative and antitumor activity.

2.6. In silico metabolism study

The metabolic stability of **10** and **25** was first examined in silico by using MetaSite[51,52] computational method in two models of metabolism: liver and CYP3A4 exclusively, and compared to the results obtained for *pitolisant*. For compound **10** the highest probability of metabolism calculated by liver model occurred at the 3-substituted position of piperidine moiety. However, for compound **25** MetaSite predicted similar to *pitolisant* highest possibility of metabolism at the aliphatic linker. The use of CYP3A4 model showed for both examined compounds (**10** and **25**) and for *pitolisant* as the most reactive position of metabolism, the methylene bridge straightly connected to nitrogen in the piperidine moiety.

Table 2
Preliminary anticonvulsant evaluation of compounds **9**–**28** in the MES, the scMET and TOX test (mice, ip)*

Compd	Dose (mg/kg)	MES[1]		scMET[2]		TOX[3]	
		0.5 h	4.0 h	0.5 h	4.0 h	0.5 h	4.0 h
9	3	0/4	–	–	–	0/4	–
	10	0/4	–	–	–	0/4	–
	30	**1/1**	0/1	0/1	0/1	0/4	0/2
	100	**2/2**	–	0/1	–	**8/8**[a,b]	–
	300	–	–	–	–	**4/4**[b]	–
10	3	0/4	–	–	–	0/4	–
	10	**1/4**	–	–	–	0/4	–
	30	**1/1**	0/1	0/1	0/1	0/4	0/2
	100	–	–	0/1	0/1	**8/8**[a,b]	–
	300	–	–	–	–	**4/4**[b]	–
11	3	0/4	–	–	–	0/4	–
	10	0/4	–	–	–	0/4	–
	30	**1/1**	**1/1**	0/1	0/1	**1/4**[f]	0/2
	100	–	–	–	–	**8/8**[b]	–
	300	–	–	–	–	**4/4**[b]	–
12	3	0/4	–	–	–	0/4	–
	10	0/4	–	–	–	0/4	–
	30	**1/1**	0/1	0/1	0/1	0/4	0/2
	100	–	**1/1**	0/1	–	**8/8**[a,b,d]	0/1
	300	–	–	–	–	**4/4**[b]	–
13	3	0/4	–	–	–	0/4	–
	10	0/4	–	–	–	0/4	–
	30	**1/1**	0/1	0/1	0/1	0/4	0/2
	100	**2/2**	**3/3**	0/1	0/1	**8/8**[a,b]	0/4
	300	–	–	–	–	**4/4**[b]	–
14	3	0/4	–	–		0/4	–
	10	0/4	–	–		0/4	–
	30	**1/1**	0/1	0/1	0/1	0/4	0/2
	100	**3/3**	**3/3**	0/1	0/1	**8/8**[a]	0/4
	300	–	–	–	–	**4/4**[b]	0/0
15	3	0/4	–	–	–	0/4	0/4
	10	0/4	–	–	–	0/4	0/4
	30	**1/1**	0/1	0/1	0/1	0/4	0/2
	100	**1/1**	**1/1**	–	–	**8/8**[a,b]	0/1
	300	–	–	–	–	**4/4**[b]	–
16	3	0/4	–	–	–	0/4	–
	10	0/4	–	–	–	0/4	–
	30	**1/1**	0/1	0/1	0/1	1/4	0/2
	100	**1/1**	–	0/1	–	**8/8**[a,b]	–
	300	–	–	–	–	**4/4**[b]	–
17	3	0/4	0/4	-	-	0/4	0/4
	10	**1/4**	0/4	-	-	0/4	0/4
	30	**1/1**	**1/1**	0/1	0/1	**1/4**	0/2
	100	–	–	–	–	**8/8**[b]	–
	300	–	–	–	–	**4/4**[b]	–
18	3	0/4	–	–	–	0/4	–
	10	0/4	–	–	–	0/4	–
	30	**1/1**	0/1	0/1	0/1	0/4	0/2
	100	**3/3**	**3/3**	0/1	0/1	0/8	0/4
	300	–	**1/1**	–	–	**4/4**[b,d]	0/1
19	3	0/4	–	–	–	0/4	–
	10	**4/4**	–	–	–	0/4	–
	30	**1/1**	**1/1**	0/1	0/1	0/4	0/2
	100	–	–	–	–	**8/8**[b]	–
	300	–	–	–	–	**4/4**[b]	–
20	3	0/4	–	–	–	0/4	–
	10	0/4	–	–	–	0/4	–
	30	**1/1**	0/1	0/1	0/1	0/4	0/2
	100	**1/1**	–	–	–	**8/8**[b,g,h]	–
	300	–	–	–	–	**4/4**[b]	–
21	30	0/1	0/1	0/1	0/1	0/4	0/2
	100	**2/3**	0/3	0/1	0/1	0/8	0/4
	300	–	–	–	–	**4/4**[b]	**1/1**[b]
22	30	0/1	0/1	0/1	0/1	0/4	0/2
	100	**3/3**	**2/2**	0/1	0/1	**8/8**[a,b]	0/3
	300	–	–	–	–	**4/4**[b]	–
23	30	0/1	0/1	0/1	0/1	0/4	0/2

Table 2 (*continued*)

Compd	Dose (mg/kg)	MES[1]		scMET[2]		TOX[3]	
		0.5 h	4.0 h	0.5 h	4.0 h	0.5 h	4.0 h
	100	**1/2**	**3/3**	0/1	0/1	**6/8**[a,b]	**2/4**
	300	**1/1**	–	–	–	**4/4**[a–c]	–
24	30	0/1	0/1	0/1	0/1	0/4	0/2
	100	**2/2**	**2/3**	–	0/1	**7/8**	0/4
	300	–	–	–	–	**4/4**	–
25	3	0/4	–	–	–	0/4	–
	10	0/4	–	–	–	0/4	–
	30	**1/1**	0/1	0/1	0/1	0/4	0/2
	100	**1/1**	**1/1**	–	–	**8/8**[a,b]	**2/3**[b]
	300	–	–	–	–	**4/4**[b]	–
26	3	0/4	0/4	–	–	0/4	0/4
	10	**1/4**	0/4	–	–	0/4	0/4
	30	**1/1**	**1/1**	0/1	0/1	0/4	0/2
	100	**3/3**	**2/2**	0/1	–	**7/8**[a–e]	0/2
	300	–	–	0/1	–	**4/4**[b,c]	–
27	3	0/4	–	–	–	0/4	–
	10	0/4	–	–	–	0/4	–
	30	**1/1**	0/1	0/1	0/1	0/4	0/2
	100	**3/3**	**3/3**	0/1	0/1	**6/8**[a,c,e]	**1/4**
	300	–	–	–	–	**4/4**[b]	–
28	3	0/4	–	–	–	0/4	–
	10	0/4	–	–	–	0/4	–
	30	**1/1**	0/1	0/1	0/1	0/4	0/2
	100	**1/1**	**2/2**	–	–	**8/8**[b,d]	**3/3**[b]
	300	–	–	–	–	**4/4**	–

– The compound was not tested in the particular case.
[a–g]Kind of toxicity: [a]unable to grasp rotarod; [b]death; [c]diarrhea; [d]loss of righting reflex; [e]clonic seizures; [f]vocalization; [g]sedated; [h]myoclonic jerks.
* Ratios where at least one animal was protected have been highlighted in bold for easier data interpretation.
[1] MES—maximum electroshock seizure: number of animals protected/number of animals tested.
[2] scMet—subcutaneous pentetrazole evoked seizure test: number of animals protected/number of animals tested.
[3] TOX—neurotoxicity assay (the rotarod test): number of animals exhibiting toxicity/number of animals tested.

Table 3
Anticonvulsant activity in the MES test in rats (ip)*

Compd	Test	Dose (mg/kg)	Pretreatment time				
			0.25 h	0.5 h	1.0 h	2.0 h	4.0 h
20	MES	30	**2/4**	**2/4**	**2/4**	**1/4**	0/4
	TOX	30	0/4	0/4	0/4	0/4	0/4
26	MES	30	**3/4**	**4/4**	**4/4**	**4/4**	**1/4**
	TOX	30	0/4	0/4	0/4	0/4	0/4

MES—maximum electroshock seizure: number of animals protected/number of animals tested.
TOX—neurotoxicity assay (the rotarod test): number of animals exhibiting toxicity/number of animals tested.
* Ratios where at least one animal was protected have been highlighted in bold for easier data interpretation.

The places of metabolism are shown in Figures 7 and 8. The circle marked the site of H_3R ligand involved in metabolism with the highest probability calculated by MetaSite method. The darker color of the marked functional group indicates its higher likelihood to be involved in the metabolic pathway.

2.7. In vitro metabolism study

The metabolic stability of compounds **10** and **25** was also determined in vitro. The examined H_3R ligands were incubated for 2 h with human liver microsomes (HLMs). A full scan chromatograms of the reaction mixtures obtained by UPLC–MS/MS detected the presence of unreacted substrates and the two metabolites of *pitolisant*, **10** and **25** each (Figs. 9–11). The mass spectra gave the accurate molecular masses of all metabolites which were up either 16 or 32 mass units in compare to the substrates, suggesting the addition of one or two oxygen atoms and in consequence one or two hydroxyl groups. To locate the site(s) of hydroxylation, the precise analysis of the fragment ions produced by substrates and metabolites under ion fragment analysis conditions were undertaken and supported by in silico data. The obtained results showed the similar metabolism pathway of *pitolisant* (metabolite M1 with $m/z = 328$ corresponding to the quasimolecular ion $[M+H]^+$; Fig. 9B) and compound **25** (metabolite M1 with $m/z = 342$ corresponding to the quasimolecular ion $[M+H]^+$; Fig. 10B). Based on the comparison of ion fragment analyses of *pitolisant* and **25** to the analysis of their aforementioned metabolites, the lack of characteristic peak coming from *N*-methyl-piperidine with $m/z = 98$ produced by substrates and the appearance of the new ion fragment with $m/z = 101$ produced by metabolites were observed. Additionally, further analysis of the another ion fragments produced by both metabolites excluded the double hydroxylation of benzene ring or at aliphatic linker of *pitolisant* and **25** suggesting rather the degradation of piperidine moiety followed by oxidation (Figs. 9A–C and 10A–C). The metabolite M2 of *pitolisant* ($m/z = 312$; Fig. 9C) was observed as a hydroxyl derivative with hydroxyl group located at the methylene bridge situated probably next to the ether bound. The site of hydroxylation was determined due to the fragment ions with $m/z = 142$ and $m/z = 125$ produced by M2, which excluded the presence of the hydroxyl group at the piperidine and benzene ring as well as at the part of aliphatic linker situated closer to the piperidine moiety (Fig. 9C). Moreover, the in silico *pitolisant* metabolism prediction by liver model showed that the methylene bridges which are nearby to the ether bound, are susceptible for the modifications (Fig. 7). The molecular mass of the another metabolite of **25** (M2) indicated the presence of one

Table 5
Results of anticonvulsant activity of tested compounds in the 6-Hz test in mice (ip)*

Com	Test	Dose (mg/kg)	Pretreatment time				
			0.25 h	0.5 h	1.0 h	2.0 h	4.0 h
13	6 Hz	50	**1/4**	0/4	0/4	0/4	0/4
	TOX	50	**3/4**	**2/4**	0/4	0/4	0/4
14	6 Hz	50	0/4	0/4	0/4	**1/4**	0/4
	TOX	50	**1/4**	0/4	0/4	0/4	0/4
15	6 Hz	50	**4/4**	**2/4**	**2/4**	**1/4**	**1/4**
	TOX	50	**2/4**	1/4	0/4	0/4	0/4
16	6 Hz	30	0/4	0/4	0/4	0/4	0/4
	TOX	30	0/4	0/4	0/4	0/4	0/4
17	6 Hz	30	0/4	0/4	0/4	0/4	0/4
	TOX	30	0/4	0/4	0/4	0/4	0/4
	6 Hz	60	**3/4**	**3/4**	**2/4**	**2/4**	0/4
	TOX	60	**3/4**	**2/4**	0/4	0/4	0/4
18	6 Hz	100	**2/3**	0/4	0/2	**2/2**	**1/3**
	TOX	100	**4/4**	**4/4**	**4/4**	**4/4**	**1/4**
19	6 Hz	25	0/4	0/4	0/4	0/4	0/4
	TOX	25	0/4	0/4	0/4	0/4	0/4
	6 Hz	50	**2/4**	**3/4**	**4/4**	0/4	0/4
	TOX	50	**3/4**	**4/4**	**2/4**	0/4	0/4
20	6 Hz	50	0/4	**1/4**	0/4	0/4	0/4
	TOX	35	**4/8**	**1/8**	—	—	—
	TOX	45	**8/8**	**8/8**	**5/8**	**1/8**	0/8
	TOX	50	**4/4**	**4/4**	**4/4**	0/4	0/4
25	6 Hz	50	0/4	0/4	**2/4**	**1/4**	0/4
	TOX	50	0/4	**1/4**	0/4	0/4	0/4
26	6 Hz	30	0/4	0/4	0/4	0/4	0/4
	TOX	30	0/4	0/4	0/4	0/4	0/4
	6 Hz	60	**2/4**	**3/4**	**2/4**	**2/4**	**1/4**
	TOX	60	**2/4**	**3/4**	0/4	0/4	0/4
28	6 Hz	50	0/4	**1/4**	**2/4**	0/4	0/4
	TOX	50	**4/4**	**3/4**	**3/4**	0/4	0/4

— The compound was not tested in the particular case.
6 Hz—psychomotor seizure test: number of animals protected/number of animals tested.
TOX—neurotoxicity assay (the rotarod test): number of animals exhibiting toxicity/number of animals tested.
* Ratios where at least one animal was protected have been highlighted in bold for easier data interpretation.

additional hydroxyl group (m/z = 326; Fig. 10C). However, in comparison to the metabolite M2 of *pitolisant* the hydroxylation of **25** occurred not at the aliphatic linker but probably at the *ortho* position of the benzene moiety (Fig. 10C). It was observed, that metabolite M2 of **25** produced two fragment ions with m/z = 98 and m/z = 182, which excluded hydroxylation at the piperidine moiety or at the aliphatic linker, and the fragment ion with m/z = 144 which confirmed the presence of hydroxyl group at the benzene moiety (Fig. 10C). Moreover, the results of **25** metabolism prediction in silico by liver model showed the higher probability of hydroxylation rather at the *ortho* than at the *meta* position of the benzene moiety (Figs. 7 and 10C).

Metabolic pathway of compound **7** included the addition of one (M1) or two (M2) hydroxyl groups (Fig. 11). According to **10** in silico metabolism prediction, the highest probability to be involved in the metabolic pathway was shown at the 3-position of piperidine moiety, probably due to the presence of the methyl substituent (Fig. 7). The ion fragment analysis of M1 showed hydroxylation of the parent ion (m/z = 312) and its major fragment (m/z = 294) corresponding to ion where the water elimination occurred (Fig. 11B). The precise study of the fragmentation routes of the parent ion as well as the major dehydrated fragment did not confirm the in silico data, which indicated the presence of the hydroxyl group at the α position to piperidine nitrogen (Figs. 7 and 11B). The molecular mass of metabolite M2 of **10** indicated the presence of two additional hydroxyl groups (m/z = 328; Fig. 11C). The sites of di-hydroxylation were determined due to the fragment ions with m/z = 98, m/z = 126 and m/z = 168 produced by M2, which excluded the presence of the hydroxyl group at the piperidine moiety or aliphatic linker (Fig. 11C). Moreover, as discussed before for **25**, the results of metabolism prediction in silico by liver model, showed the higher probability of hydroxylation of **7** at the *ortho* than at the *meta* position of the benzene moiety (Figs. 7 and 11C).

The luminescent CYP3A4 P450-Glo™ assay was also used for testing the effects compounds **10** and **25** on CYP3A4 activities. As it is shown in Figure 12, compounds **10**, **25** and *pitolisant* did not modulate cytochrome activity up to 10 μM, whereas the reference compound ketoconazole inhibited completely the CYP3A4 at 10 μM.

3. Conclusions

In this series of compounds, structures with promising submicromolar affinity were obtained. Although, changing of place of the ether function in investigated group of chlorophenoxyalkyl

Table 6
Quantitative anticonvulsant data in mice and/or rats (ip)

Compd	Animals	MES ED_{50} (mg/kg) (95% confidence interval)	scMET ED_{50} (mg/kg)	TOX TD_{50} (mg/kg) (95% confidence interval)	PI TD_{50}/ED_{50}
18	Mice	16.80[a] (13.3–19.3)	>50[a]	50.40[a] (45.4–57.4)	3
19	Mice	13.04[b] (11.31–15.16)	>30[b]	40.77[a] (39.4–41.8)	3.1
20	Rats	14.00[a] (8.4–18.7)	>44[a]	44.10[a] (38.3–48.5)	3.2
26	Mice	16.14[a] (14.89–17.3)	>47[a]	48.28[a] (45.6–52.1)	3
	Rats	13.18[c] (8.06–18.78)	>50[b]	50.35[b] (45.7–55.8)	3.8
Lamotrigine[d]	Mice	7.47 (6.13–9.11)	>40	30 (24.8–36.2)	4.0
Phenobarbital[d]	Mice	21.8 (15.0–25.5)	13.2 (5.87–15.9)	69.0 (62.8–72.9)	3.2^{MES} 5.2^{scMET}
Valproic acid[d]	Mice	263 (237–282)	220 (177–268)	398 (356–445)	1.5^{MES} 1.8^{scMET}

[a] Results observed after 0.25 h of administration of compound.
[b] Results observed after 0.5 h of administration of compound.
[c] Results observed after 1 h of administration of compound.
[d] Data from Ref. 37.

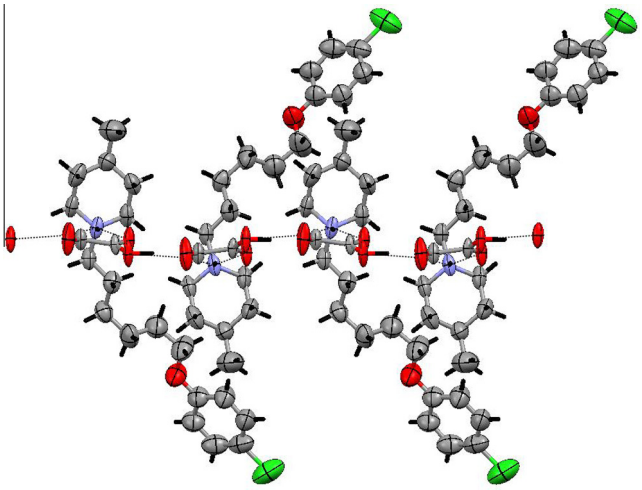

Figure 3. ORTHEP drawing of **19** hydrogen oxalate structure (light grey color for carbons, red for oxygen, blue for nitrogen and green for chlorine).

derivatives (as compared to *pitolisant*) significantly influence the affinity of the examined compounds toward hH_3R. The highest affinities were observed for 4-chloro substituted derivatives: **10** and **25** (K_i = 133 and 128 nM, respectively) with five and seven carbons alkyl chain. Also, the character of cyclic amine had a huge influence on the affinity of the evaluated compounds—generally, for this group the most potent were 3-methylpiperidine derivatives. The results of anticonvulsant screening revealed that all of the synthesized compounds showed activity in the MES screen (mice; ip). Two compounds **20** and **26** were especially promising and were also tested in different models of epilepsy (e.g., 6 Hz test, corneal kindled in mice, pilocarpine in rats). Quantitative assays for **20** and **26** in mice (ip) and/or rats (ip) provided an evaluation of the ED_{50} values. The highest activity was observed for **20** with ED_{50} of 14 mg/kg (MES; mice) and **26** with ED_{50} of 16.14 mg/kg (MES; mice) and with ED_{50} of 13.18 mg/kg (MES; rats). Moreover, the examined compounds show satisfying, selected ADME-TOX parameters.

4. Experimental

4.1. Chemistry

All reagents were purchased from commercial suppliers and were used without further purification. *Pitolisant* was synthesized by us in the Department of Technology and Biotechnology of Drugs (Kraków, Poland) as described by Meier et al.[53] Melting points (mp) were determined on a MEL-TEMP II (LD Inc., USA) melting point apparatus and are uncorrected. IR spectra were measured as KBr pellets on FT Jasco IR spectrometer. UV spectra were recorded on a Jasco UV/Vis V-530 apparatus in 10^{-5} mol/L in methanol. Mass spectra (LC/MS) were performed on Waters TQ Detector mass spectrometer. ^{1}H NMR spectra were recorded on a Varian Mercury 300 MHz PFG spectrometer in DMSO-d_6 or a Bruker AMX 300 (300 MHz) spectrometer (Bruker, Germany) in DMSO-d_6. Chemical shifts were expressed in parts per million (ppm) using the solvent signal as an internal standard. Data are reported in the following order: multiplicity (s, singlet; d, doublet; t, triplet; q, quartet; qu, quintet, m, multiplet; br, broad; cPropPh, phenyl; Pip, piperidine; hPip, homopiperidine), approximate coupling constants J expressed in Hertz (Hz), number of protons. ^{13}C NMR spectra were recorded on Varian-Mercury-VX 300 MHz PFG or 400 MHz spectrometer in DMSO-d_6. LC–MS were carried out on a system consisting of a Waters Acquity UPLC, coupled to a Waters TQD mass spectrometer. Retention times (t_R) are given in minutes. The UPLC/MS purity of all final compounds was determined (%). Elemental analyses (C, H, N) were performed on an Elemental Analyser Vario El III (Hanau, Germany) and agreed with theoretical values within ±0.4%. TLC data were obtained with Merck silica gel $60F_{254}$ aluminum sheets with the following detection with UV light and evaluation with Dragendorff's reagent (solvent system: methylene chloride/methanol 9:1). RP-TLC data were obtained with Merck Silica gel 60 RP-18 $F_{254}S$ glass plates, using planar chromatographic CHROMDES chambers. Compounds solutions were applied using Hamilton 25 μL syringes. Detection of compounds was obtained by the staining of TLC plates with iodine vapors. For CC (column chromatography) using silica gel 60 (0.063–0.20 mm; Merck) solvent systems were used: I: CH_2Cl_2; II: CH_2Cl_2/MeOH (9:1).

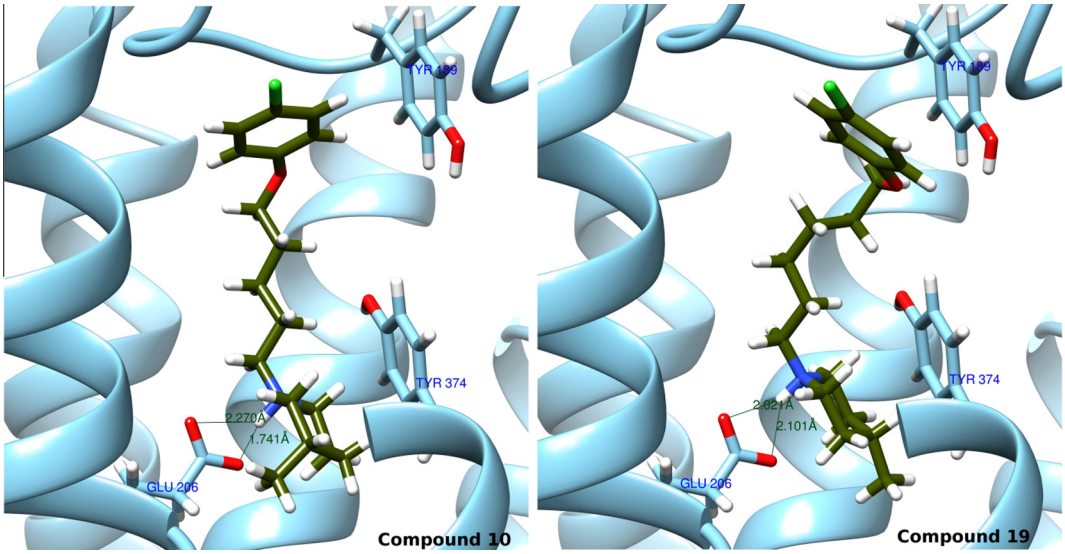

Figure 4. Position of compounds **10** and **19** in the binding pocket of H_3R (ligand: white color for hydrogens, dark green for carbons, blue for nitrogen, light green for chlorine. Green lines represent salt bridges).

Table 8
Practical (R_{M0}) and theoretical lipophilicity values for the series of described compounds

No.	R_{M0}	QikProp[a]	Chem3D[b]	Marvin[c]
9	0.914	4.513	5.187	0.81
10	0.994	4.925	5.537	1.17
11	0.993	4.914	5.537	1.17
12	0.921	4.848	5.746	1.25
13	0.99	4.910	5.716	1.25
14	1.202	4.870	6.065	1.62
15	1.203	5.295	6.065	1.62
16	1.115	5.074	6.275	1.70
17	0.99	4.962	5.716	1.25
18	1.203	5.297	6.065	1.62
19	1.202	5.292	6.065	1.62
20	1.115	5.025	6.275	1.70
21	1.059	5.359	6.245	1.70
22	1.504	5.548	6.594	2.06
23	1.503	5.714	6.594	2.06
24	1.473	5.711	6.804	2.14
25	1.059	5.293	6.245	1.70
26	1.505	5.674	6.594	2.06
27	1.504	5.722	6.594	2.06
28	1.479	5.609	6.804	2.14

[a] Ref. 44.
[b] Ref. 48.
[c] Ref. 49.

4.1.1. General procedure for compounds 4–8*

*Compounds **4**,[54–56] **6**[56] and **8**[57] were obtained previously but in the different conditions.

To a solution of freshly prepared sodium propanolate (50 mL; 1.15 g, 0.05 mol Na), proper substituted phenols were added and stirred in room temperature (RT) for 15 min. α,ω-dibromoalkanes were then added dropwisely in the time of one hour. The reaction mixture was stirred in 60 °C for 3 h, and then refluxed for another 3 h. After cooling down to RT reaction mixture was filtrated and evaporated. To a crude product, 100 mL of 10% NaOH was added and left overnight in cold. To a resulting white oil, CH_2Cl_2 was added, mixed and layers were then separated. Organic layer was dried over sodium sulphate filtered and evaporated. Used without further purification (**4**, **6**, **8**) or purified by Flash Chromatography (FC; **5**, **7**) (petroleum ether/CH_2Cl_2 [95:5]).

4.1.2. 1-((5-Bromopentyl)oxy)-4-chlorobenzene (4)[54–56]

Synthesis from 4-chlorophenol (6.4 g, 0.05 mol), 1,5-dibromopentane (11.5 g, 0.05 mol) in sodium propanolate (50 mL propan-1-ol, 1.15 g, 0.05 mol Na). Obtained 8.8 g of crude product. Yield 63%.

4.1.3. 1-((6-Bromohexyl)oxy)-3-chlorobenzene (5)

Synthesis from 3-chlorophenol (6.4 g, 0.05 mol), 1,6-dibromohexane (12.2 g, 0.05 mol) in sodium propanolate (50 mL propan-1-ol, 1.15 g, 0.05 mol Na). Obtained 4.7 g after purification by FC. Yield 32%.

^{1}H NMR (DMSO-d_6) δ: 7.27 (t, J = 8.0 Hz, 1H, Ph-5-*H*), 6.91–7.01 (m, 2H, Ph-2,4-*H*), 6.87 (dd, J = 1.7, 8.3 Hz, 1H, Ph-6-*H*), 3.95 (t, J = 6.4 Hz, 2H, CH_2-O), 3.51 (t, J = 6.7 Hz, 2H, CH_2-Br), 1.79 (quin, J = 6.80 Hz, 2H, —O-CH_2-CH_2—), 1.68 (quin, J = 6.5 Hz, 2H, —CH_2-CH_2-Br), 1.31–1.50 (m, 4H, 2 × —CH_2—); ^{13}C NMR (300 MHz, DMSO-d_6) δ: 160.06, 134.16, 131.24, 120.76, 114.84, 113.97, 68.16, 35.51, 32.62, 28.81, 27.70, 25.05.

4.1.4. 1-((6-Bromohexyl)oxy)-4-chlorobenzene (6)[56]

Synthesis from 4-chlorophenol (3.2 g, 0.025 mol), 1,6-dibromohexane (6.1 g, 0.025 mol) in sodium propanolate (25 mL propan-1-ol, 0.575 g, 0.025 mol Na). Obtained 5.4 g of crude product. Yield 74%.

4.1.5. 1-((7-Bromoheptyl)oxy)-3-chlorobenzene (7)

Synthesis from 3-chlorophenol (3.2 g, 0.025 mol), 1,7-dibromoheptane (6.45 g, 0.025 mol) in sodium propanolate (25 mL propan-1-ol, 0.575 g, 0.025 mol Na). Obtained 2.6 g after purification by FC. Yield 34%.

^{1}H NMR (300 MHz, DMSO-d_6) δ: 7.26 (t, J = 8.1 Hz, 1H, Ph-5-*H*), 6.91–7.01 (m, 2H, Ph-2,4-*H*), 6.87 (dd, J = 1.5, 8.5 Hz, 1H, Ph-6-*H*), 3.95 (t, J = 6.4 Hz, 2H, CH_2-O), 3.50 (t, J = 6.7 Hz, 2H, CH_2-Br), 1.78 (quin, J = 6.8 Hz, 2H, —O-CH_2-CH_2—), 1.67 (def quin, 2H, —CH_2-CH_2-Br), 1.26–1.45 (m, 6H, 3 × CH_2—); ^{13}C NMR (300 MHz, DMSO-d_6) δ: 160.08, 134.16, 131.24, 120.74, 114.82, 113.97, 68.21, 35.57, 32.63, 28.23, 27.90, 25.72.

4.1.6. 1-((7-Bromoheptyl)oxy)-4-chlorobenzene (8)[57]

Synthesis from 4-chlorophenol (6.4 g, 0.05 mol), 1,7-dibromoheptane (12.9 g, 0.05 mol) in sodium propanolate (50 mL propan-1-ol, 1.15 g, 0.05 mol Na). Obtained 11.3 g of crude product. Yield 74%.

4.1.7. General procedure for compounds 9–28

To a suspension of potassium carbonate and catalytic amount of potassium iodide in water, a proper cyclic amine and compounds **4**–**8** in ethanol were added. Mixture was then refluxed for 20 h (TLC controlled). After cooling down to RT, the solid was filtrated and the residue evaporated under the reduced pressure and purified by one of procedures:

Procedure A: To a resulting oil, 100 mL of CH_2Cl_2 was added and washed with: 0.5% HCl solution, 0.5% NaOH solution and water.

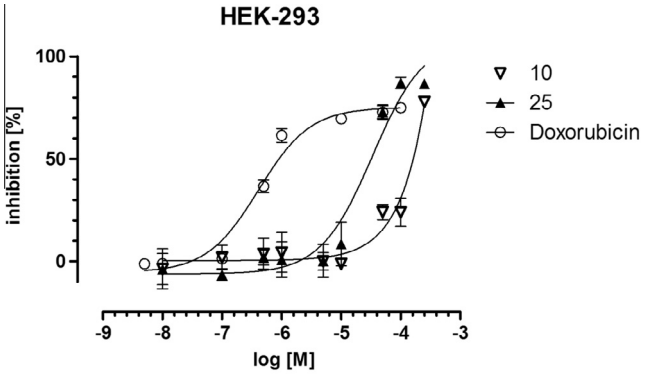

Figure 5. The antiproliferative effect of **10**, **25** and doxorubicin (reference) against HEK-293 cell line. Values represent the mean of n = 4 experiments.

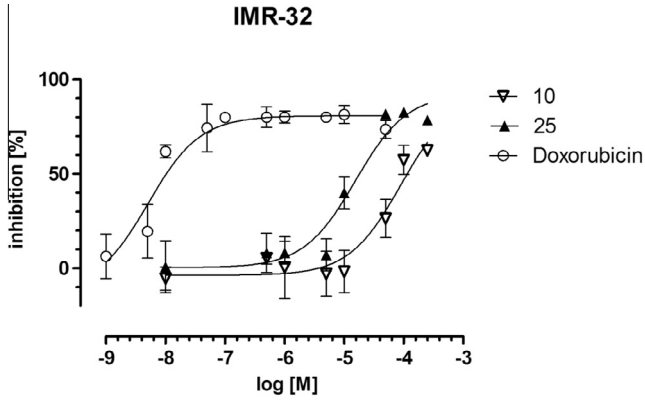

Figure 6. The antiproliferative effect of **10**, **25** and doxorubicin against IMR-32 cell line. Values represent the mean of n = 4 experiments.

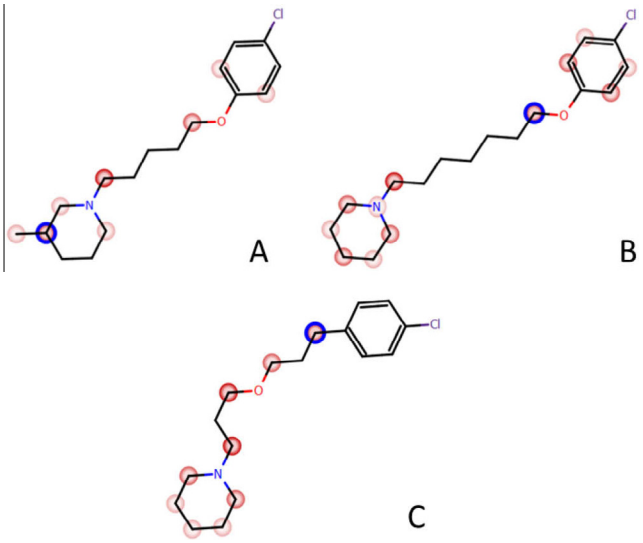

Figure 7. Plots of MetaSite predictions for sites of metabolism for **10** (A), **25** (B) and *pitolisant* (C) by liver. The darker color of the marked functional group indicates its higher probability to be involved in the metabolic pathway. The blue circle marked the site of H_3R ligand involved in metabolism with the highest probability calculated by MetaSite method.

Organic layer was evaporated and dissolved in 3% HCl solution, followed by washing with diethyl ether and neutralization with 10% NaOH solution. Final product was extracted with CH_2Cl_2 from the basic solution, dried over Na_2SO_4, filtered and evaporated.

Procedure B: Column chromatography ($MeOH/CH_2Cl_2$; 9:1).

Oily products (from procedure A or B) were transformed into oxalic acid salts using 10% excess of oxalic acid solution in absolute ethanol in RT, and then precipitated by addition of ethyl ether.

4.1.8. 1-(5-(4-Chlorophenoxy)pentyl)piperidine hydrogen oxalate (9)

Synthesis from **4** (1.39 g, 0.005 mol) and piperidine (0.85 g, 0.01 mol), K_2CO_3 (2.07 g, 0.015 mol), KI (catalytic amount) in ethanol (105 mL) and water (20 mL). Obtained 0.7 g of oil. Purified by procedure A. Yield 50%. Raw product was transformed into oxalic acid salt yielding 0.82 g of final compound. Mp: 134–136 °C. [1-(5-(4-Chlorophenoxy)pentyl)piperidine hydrochloride, mp. 178–180 °C).[34]] $C_{16}H_{24}NOCl \times C_2H_2O_4$ (MW = 371.19). ^1H NMR (DMSO-d_6) δ: 7.31 (d, J = 9.2 Hz, 2H, Ph-3,5-*H*), 6.93 (d, J = 9.0 Hz, 2H, Ph-2,6-*H*), 3.94 (t, J = 6.3 Hz, 2H, CH_2-O), 3.27–2.91 (m, 6H, Pip-2,6-H_2 + Pip-CH_2), 1.75–1.61 (m, 8H, Pip-3,5-H_2, 2CH_2), 1.50–1.34 (m, 4H, Pip-4-H_2, —CH_2). ^{13}C NMR (400 MHz, DMSO-d_6) δ: 165.20, 157.91, 129.66, 124.54, 116.64, 67.92, 56.21, 52.24, 28.49, 23.35, 23.22, 22.97, 21.99. UV–VIS, λ_{max} (log ε): 217 (4.24), 224 (4.26), 227 (4.28), 281 (4.16). LC–MS: purity 100% t_R = 4.94, (ESI) m/z $[M+H]^+$ 282.23. IR (cm^{-1}): 3422.06 ($N(CH_2—)_3$), 3030.59 (aromatic CH=), 2944.77 (het. CH_2—), 2864.74, 2677.68, 2546.54, 1718.26, 1646.91, 1491.67, 1249.79 (O-CH aromatic), 1091.51, 1015.34, 946.88, 857.20, 720.28 (alif. CH_2—). Anal. calcd for $C_{16}H_{24}NOCl \times C_2H_2O_4$: C, 58.24; H, 7.06; N, 3.77. Found: C, 58.05; H, 7.22; N, 3.75.

4.1.9. 1-(5-(4-Chlorophenoxy)pentyl)-3-methylpiperidine hydrogen oxalate (10)

Synthesis from **4** (1.39 g, 0.005 mol) and 3-methylpiperidine (0.99 g, 0.01 mol), K_2CO_3 (2.07 g, 0.015 mol), KI (catalytic amount) in ethanol (105 mL) and water (20 mL). Obtained 0.8 g of oil. Purified by procedure A. Yield 54%. Raw product was transformed into oxalic acid salt yielding 0.93 g of final compound. Mp: 119–121 °C. $C_{17}H_{26}NOCl \times C_2H_2O_4$ (MW = 385.90) ^1H NMR (DMSO-d_6) δ: 7.29 (d, J = 8.7 Hz, 2H, Ph-3,5-*H*), 6.93 (d, J = 8.7 Hz, 2H, Ph-2,6-*H*), 3.94 (t, J = 6.2 Hz, 2H, CH_2-O), 3.31 (t, J = 6.2 Hz, 2H, Pip-2,6-CH_{2a}), 2.95 (t, J = 6.1 Hz, 2H, Pip-CH_2), 2.64–2.71 (m, 1H, Pip-2-H_e), 2.49–2.38 (m, 1H, Pip-6-H_e), 1.84–1.66 (m, 8H, 3 × CH_2, Pip-5-H_2), 1.44–1.34 (m, 2H, Pip-4-H_2), 1.08–0.99 (m, 1H, Pip-3-*H*), 0.96(d, J = 6.7 Hz, 3H, CH_3). ^{13}C NMR (400 MHz, DMSO-d_6) δ: 165.27, 157.91, 129.66, 124.54, 116.64, 67.92, 57.83, 56.22, 51.86, 30.56, 28.86, 28.49, 23.35, 23.23, 22.60, 19.05. UV–VIS λ_{max} (log ε): 211 (4.29), 214 (4.31), 217 (4.32), 220 (4.33), 223 (4.33), 229 (4.32), 282 (4.19). IR (cm^{-1}): 3422.06 ($N(CH_2—)_3$), 3009.37 (aromatic CH=), 2939.95 (het. CH_2—), 2874.38 (CH_3—), 2673.68, 2556.18, 1720.19, 1637.27, 1492.63, 1474. 31, 1402.96, 1280.50, 1242.90 (O-CH aromatic), 1092.48, 1028.84, 824.42, 720.28 (alif. CH_2—). LC–MS: purity 100% t_R = 5.26, (ESI) m/z $[M+H]^+$ 296.32. Anal. calcd for $C_{17}H_{26}NOCl \times C_2H_2O_4$: C, 59.14; H, 7.31; N, 3.63. Found: C, 59.10; H, 7.53; N, 3.60.

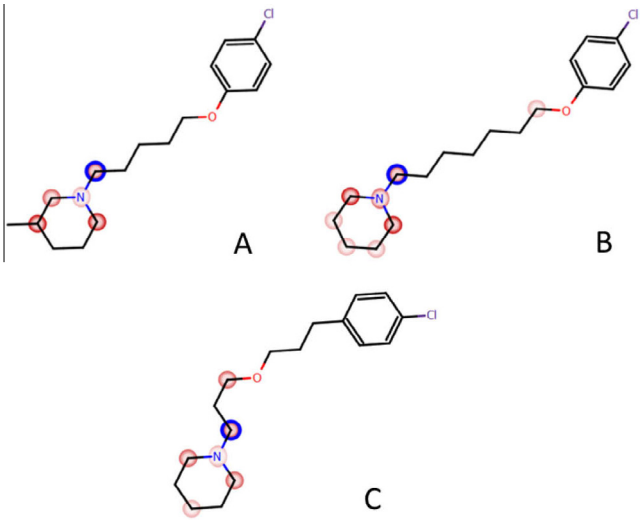

Figure 8. Plots of MetaSite predictions for sites of metabolism for **10** (A), **25** (B) and *pitolisant* (C) by CYP3A4. The darker color of the marked functional group indicates its higher probability to be involved in the metabolism pathway. The blue circle marked the site of H_3R ligand involved in metabolism with the highest probability calculated by MetaSite method.

4.1.10. 1-(5-(4-Chlorophenoxy)pentyl)-4-methylpiperidine hydrogen oxalate (11)

Synthesis from **4** (1.39 g, 0.005 mol) and 4-methylpiperidine (0.99 g, 0.01 mol), K_2CO_3 (2.07 g, 0.015 mol), KI (catalytic amount) in ethanol (105 mL) and water (20 mL). Obtained 0.8 g of oil. Purified by procedure A. Yield 54%. Raw product was transformed into oxalic acid salt yielding 0.88 g of final compound. Mp: 125–127 °C. $C_{17}H_{26}NOCl \times C_2H_2O_4$ (MW = 385.90). ^1H NMR (DMSO-d_6) δ: 7.30 (d, J = 8.7 Hz, 2H, Ph-3,5-*H*), 6.93 (d, J = 8.7 Hz, 2H, Ph-2,6-*H*), 3.94 (t, J = 6.2 Hz, 2H, CH_2-O), 3.34 (br d, J = 12 Hz, 2H, Pip-2,6-H_{2a}), 2.95 (t, J = 6.1 Hz, 2H, Pip-CH_2), 2.83–2.76 (m, 2H, Pip-2,6-H_e), 1.75–1.60 (m, 7H, 3 × CH_2, Pip-4-*H*), 1.44–1.27 (m, 4H, Pip-3,5-H_2), 0.90 (d, J = 6.4 Hz, 3H, CH_3). ^{13}C NMR (300 MHz, DMSO-d_6) δ: 165.24, 157.88, 129.65, 124.51, 116.60, 67.88, 28.46, 23.45, 23.20, 21.29. UV–VIS, λ_{max} (log ε): 215 (4.31), 218 (4.32), 222 (4.32), 225 (4.33), 281 (4.19). IR (cm^{-1}): 3430.74 ($N(CH_2—)_3$), 3019.01 (aromatic CH=), 2956.34 (het. CH_2—), 2930.31, 2866.67 (CH_3—), 2752.90, 2703.71, 2544.61, 1716.34, 1655.59, 1596.77, 1577.49, 1475.28, 1455.99, 1394.28, 1282.43, 1248.68 (O-CH aromatic), 1092.48, 1024.98, 824.42, 755.96 (alif. CH_2—). LC–MS: purity 100% t_R = 5.25, (ESI) m/z $[M+H]^+$ 296.32. Anal. calcd for $C_{17}H_{26}NOCl \times C_2H_2O_4$: C, 59.14; H, 7.31; N, 3.63. Found: C, 59.31; H, 7.45; N, 3.62.

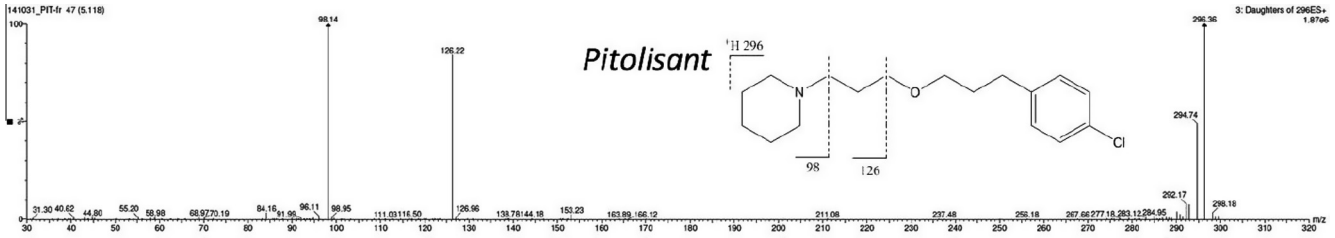

Figure 9A. MS/MS spectra and ion fragments analysis of *pitolisant*.

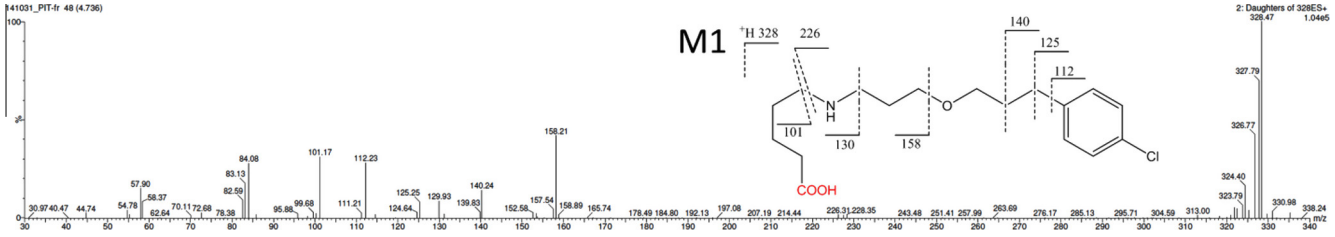

Figure 9B. MS/MS spectra and ion fragments analysis of metabolite M1 of *pitolisant* in the total ion chromatogram.

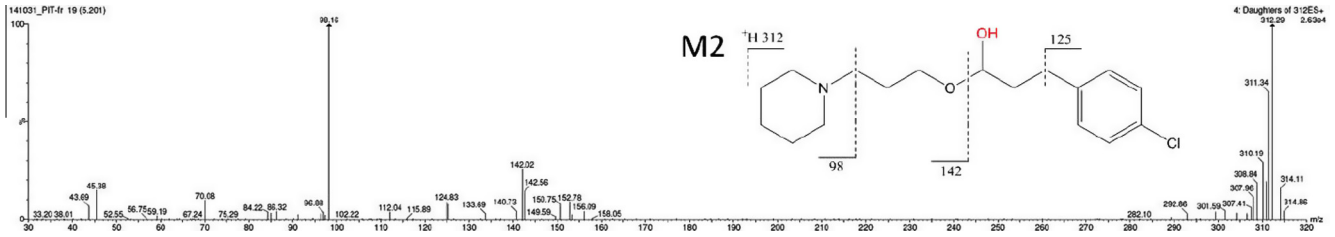

Figure 9C. MS/MS spectra and ion fragments analysis of metabolite M2 of *pitolisant* in the total ion chromatogram.

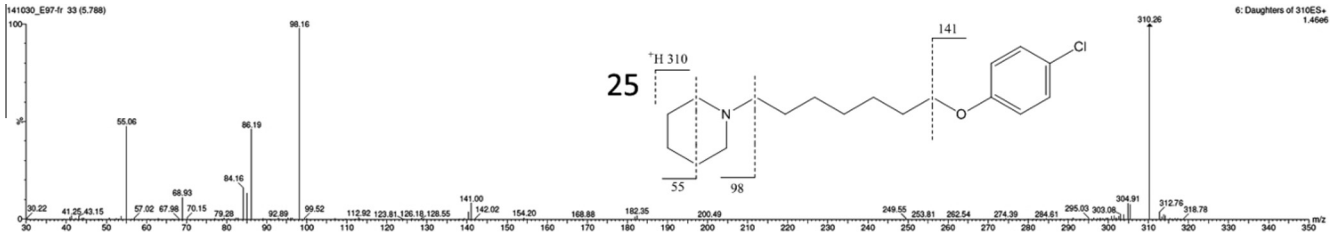

Figure 10A. MS/MS spectra and ion fragments analysis of **25** and its metabolites in the total ion chromatogram.

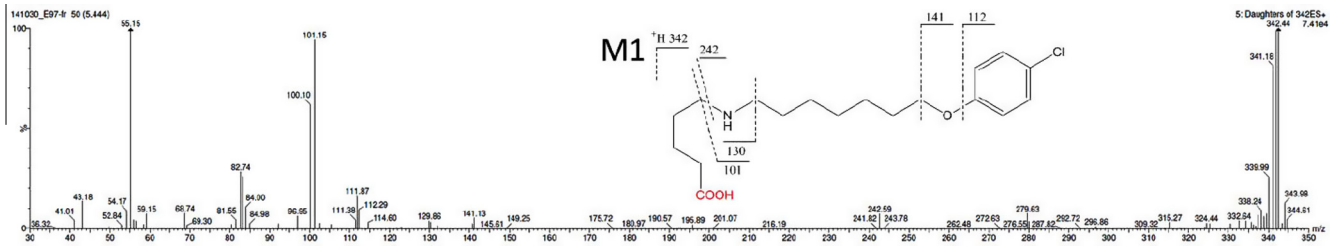

Figure 10B. MS/MS spectra and ion fragments analysis of metabolite M1 of **25** in the total ion chromatogram.

4.1.11. 1-(5-(4-Chlorophenoxy)pentyl)homopiperidine hydrogen oxalate (12)

Synthesis from **4** (1.39 g, 0.005 mol) and homopiperidine (0.99 g, 0.01 mol), K_2CO_3 (2.07 g, 0.015 mol), KI (catalytic amount) in ethanol (105 mL) and water (20 mL). Obtained 0.88 g of oil. Purified by procedure A. Yield 59%. Raw product was transformed into oxalic acid salt yielding 0.93 g of final compound. Mp: 114–116 °C. $C_{16}H_{24}NOCl \times C_2H_2O_4$ (MW = 385.90). ^{1}H NMR (DMSO-d_6) δ: 7.30 (d, J = 8.7 Hz, 2H, Ph-3,5-*H*), 6.93 (d, J = 8.7 Hz, 2H, Ph-2,6-*H*), 3.94 (t, J = 6.2 Hz, 2H, CH_2-O), 3.17 (br s, 2H, hPip-2,6-H_2), 3.02 (def t, 2H, hPip-CH_2), 1.75–1.57 (m, 8H, hPip-(3–6)-H_2), 1.64–1.54 (m, 4H, 2 × CH_2), 1.40 (def qu, 2H, CH_2). ^{13}C NMR

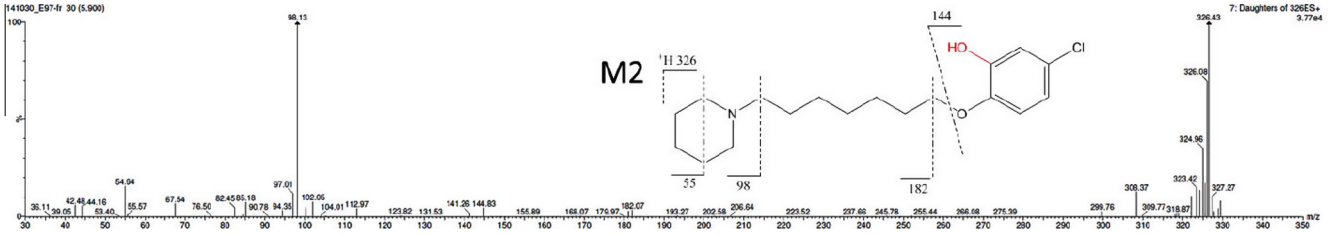

Figure 10C. MS/MS spectra and ion fragments analysis of metabolite M2 of **25** in the total ion chromatogram.

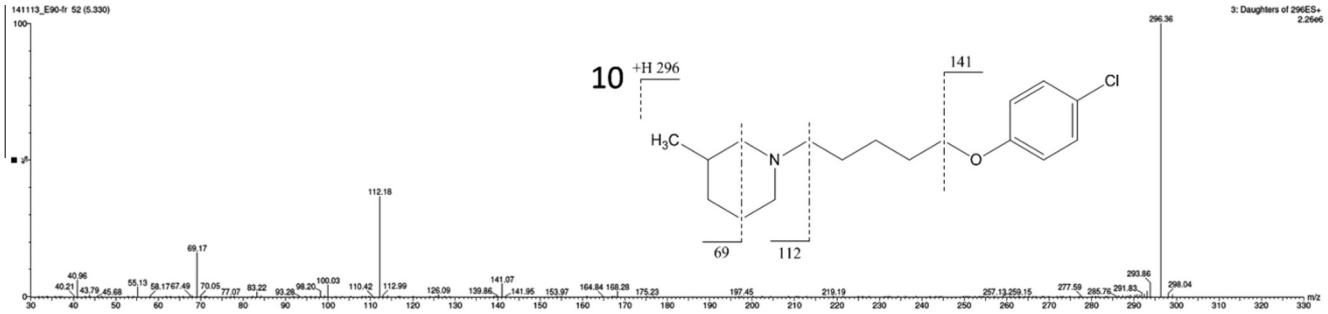

Figure 11A. MS/MS spectra and ion fragments analysis of **10** in the total ion chromatogram.

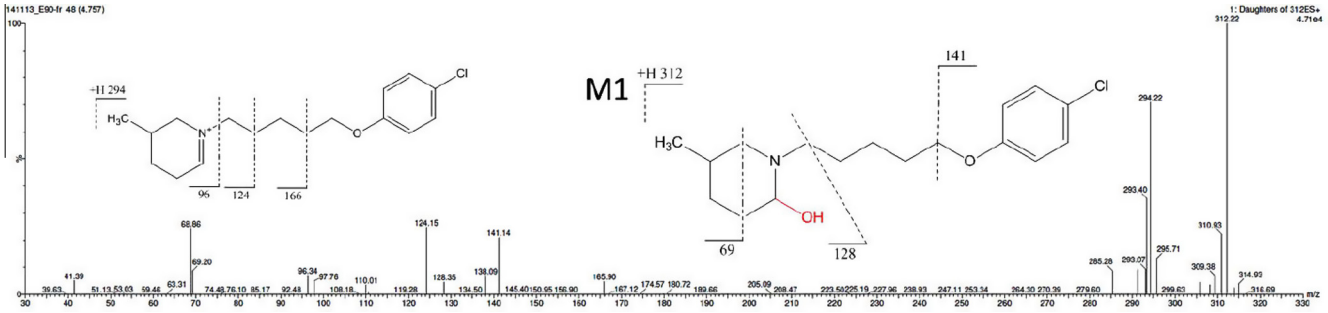

Figure 11B. MS/MS spectra and ion fragments analysis of M1 metabolite of **10** in the total ion chromatogram.

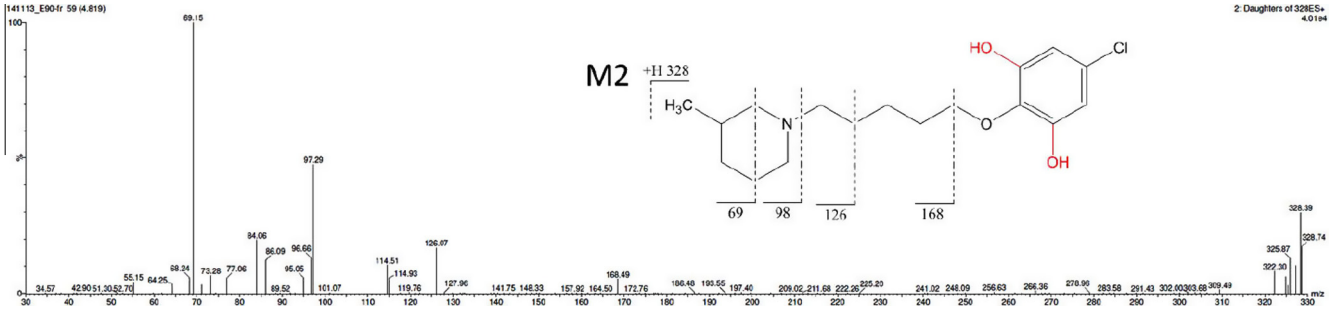

Figure 11C. MS/MS spectra and ion fragments analysis of M2 metabolite of **10** in the total ion chromatogram.

(400 MHz, DMSO-d_6) δ: 165.30, 157.91, 129.66, 124.54, 116.65, 67.95, 56.57, 53.91, 28.50, 26.55, 23.77, 23.42, 23.23. UV–VIS: λ_{max} ($\log\varepsilon$): 225 (4.29), 228 (4.29), 281 (4.14), 398 (2.62). IR (cm^{-1}): 3445.21 (N(CH_2—)$_3$), 3036.37 (aromatic CH=), 2939.95 (het. CH_2—), 2866.67, 2699.85, 2632.36, 2570.65, 2533.04, 1718.26, 1701.87, 1597.73, 1578.45, 1491.67, 1402.96, 1242.90 (O-CH aromatic), 1169.62, 1104.48, 1004.73, 825.38, 720.38 (alif. CH_2—), 668.21. LC–MS: purity 98.46% t_R = 5.23, (ESI) m/z $[M+H]^+$ 296.26. Anal. calcd for $C_{16}H_{24}NOCl \times C_2H_2O_4$: C, 59.14; H, 7.31; N, 3.63. Found: C, 59.36; H, 7.67 N, 3.55.

4.1.12. 1-(6-(3-Chlorophenoxy)hexyl)piperidine hydrogen oxalate (13)

Synthesis from **5** (1.46 g, 0.005 mol) and piperidine (0.85 g, 0.01 mol), K_2CO_3 (2.07 g, 0.015 mol), KI (catalytic amount) in ethanol (105 mL) and water (20 mL). Obtained 0.6 g of oil. Purified by procedure A. Yield 41%. Raw product was transformed into oxalic acid salt yielding 0.72 g of final compound. Mp: 109–111 °C. $C_{17}H_{26}NOCl \times C_2H_2O_4$ (MW = 385.89). ^{1}H NMR (DMSO-d_6) δ: 7.30 (t, J = 8.7 Hz, 1H, Ph-5-*H*), 6.99–6.95 (m, 2H, Ph-2,4-*H*), 6.92–6.88 (m, 1H, Ph-6-*H*), 3.98 (t, J = 6.2 Hz, 2H, CH_2-O), 3.07 (br s, 4H,

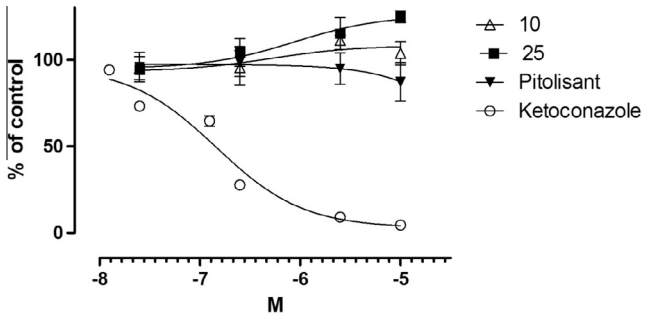

Figure 12. The effect of **10**, **25**, *pitolisant* and ketoconazole on CYP3A4 activity. Values represent the mean of $n = 3$ experiments.

Pip-2,6-CH_2), 2.94 (t, J = 6.1 Hz, 2H, N-CH_2), 1.75–1.59 (m, 8H, 2 × CH_2, Pip-3,5-H_2), 1.52–1.30 (m, 6H, 2 × CH_2, Pip-4-H_2). ^{13}C NMR (300 MHz, DMSO-d_6) δ: 165.24, 160.05, 134.15, 131.29, 120.78, 114.81, 113.99, 68.12, 59.26, 52.34, 28.70, 26.29, 25.44, 23.52, 22.94, 21.96. UV–VIS λ_{max} (log ε): 212 (4.25), 215 (4.27), 219 (4.28), 226 (4.27), 275 (4.19), 282 (4.13). IR (cm^{-1}): 3431.71 (N(CH$_2$—)$_3$), 3025.76 (aromatic CH=), 2944.77 (het. CH$_2$—), 2862.81, 2643.93, 2541.72, 1718.26, 1701.87, 1596.77, 1482.99, 1469.49, 1397.17 1334.50, 1281.47, 1243.86 (O-CH aromatic), 1097.30, 1066.48, 1032.69, 948.98, 883.24, 720.28 (alif. CH$_2$—), 684.61. LC–MS: purity 100% t_R = 5.36, (ESI) m/z [M+H]$^+$ 296.26. Anal. calcd for $C_{17}H_{26}NOCl \times C_2H_2O_4$: C, 59.14; H, 7.31; N, 3.63. Found: C, 59.40; H, 7.46 N, 3.62.

4.1.13. 1-(6-(3-Chlorophenoxy)hexyl)-3-methylpiperidine hydrogen oxalate (14)

Synthesis from **5** (1.46 g, 0.005 mol) and 3-methylpiperidine (0.99 g, 0.01 mol), K_2CO_3 (2.07 g, 0.015 mol), KI (catalytic amount) in ethanol (105 mL) and water (20 mL). Obtained 0.5 g of oil. Purified by procedure A. Yield 32%. Raw product was transformed into oxalic acid salt yielding 0.54 g of final compound. Mp: 110–113 °C. $C_{18}H_{28}NOCl \times C_2H_2O_4$ (MW = 399.92). ^{1}H NMR (DMSO-d_6) δ: 7.31 (t, J = 8.7 Hz, 1H, Ph-5-H), 6.99–6.95 (m, 2H, Ph-2,4-H), 6.92–6.88 (m, 1H, Ph-6-H), 3.98 (t, J = 6.2 Hz, 2H, CH_2-O), 3.37–3.27 (m, 2H, Pip-2,6-CH_{2a}), 2.95 (t, J = 6.1 Hz, 2H, Pip-CH_2), 2.73–2.66 (m, 1H, Pip-2-H_e), 2.51–2.57 (m, 1H, Pip-6-H_e), 1.75–1.50 (m, 8H, 2 × CH_2, Pip-4,5-CH_2), 1.47–1.30 (m, 4H, 2 × CH_2), 1.11–0.97 (m, 1H, Pip-3-H), 0.88 (d, J = 6.6 Hz, 3H, CH_3). ^{13}C NMR (300 MHz, DMSO-d_6) δ: 165.26, 160.05, 134.15, 131.29, 120.78, 114.82, 113.99, 68.12, 57.80, 56.30, 51.84, 30.56, 28.87, 28.70, 26.30, 25.44, 23.56, 22.61, 19.05. UV–VIS λ_{max} (log ε): 213 (4.26), 216 (4.26), 223 (4.28), 275 (4.19), 282 (4.13). IR (cm^{-1}): 3421.10 (N(CH$_2$—)$_3$), 3024.80 (aromatic CH=), 2940.91 (het. CH$_2$—), 2866.67 (CH$_3$—), 2674.48, 2554.25, 2348.87, 1720.19, 1596.77, 1471.42, 1428.99, 1395.25, 1334.50, 1310.39, 1283.39, 1249.65 (O-CH aromatic), 1231.11, 1100.19, 1024.02, 883.24, 683.64 (alif. CH$_2$—). LC–MS: purity 100% t_R = 5.73, (ESI) m/z [M+H]$^+$ 310.28. Anal. calcd for $C_{18}H_{28}NOCl \times C_2H_2O_4$: C, 60.07; H, 7.56; N, 3.50. Found: C, 59.94; H, 7.93 N, 3.70.

4.1.14. 1-(6-(3-Chlorophenoxy)hexyl)-4-methylpiperidine hydrogen oxalate (15)

Synthesis from **5** (1.46 g, 0.005 mol) and 4-methylpiperidine (0.99 g, 0.01 mol), K_2CO_3 (2.07 g, 0.015 mol), KI (catalytic amount) in ethanol (105 mL) and water (20 mL). Obtained 0.47 g of oil. Purified by procedure A. Yield 30%. Raw product was transformed into oxalic acid salt yielding 0.54 g of final compound. Mp: 144–146 °C. $C_{18}H_{28}NOCl \times C_2H_2O_4$ (MW = 399.92). ^{1}H NMR (DMSO-d_6) δ: 7.29 (t, J = 8.7 Hz, 1H, Ph-5-H), 6.99–6.95 (m, 2H, Ph-2,4-H), 6.92–6.88 (m, 1H, Ph-6-H), 3.98 (t, J = 6.2 Hz, 2H, CH_2-O), 3.37–3.33 (m, 2H, Pip-2,6-CH_{2a}), 2.97–2.92 (m, 2H, Pip-CH_2), 2.86–2.78 (m, 2H, Pip-2,6-H_e), 1.77–1.59 (m, 7H, CH_2, Pip-3,4,5-CH), 1.47–1.30 (m, 6H, 3 × CH_2), 0.91 (d, J = 6.4 Hz, 3H, CH_3). ^{13}C NMR (400 MHz, DMSO-d_6) δ: 165.19, 160.08, 134.18, 131.31, 120.81, 114.86, 114.02, 68.16, 28.73, 28.54, 26.34, 25.47, 23.81. UV–VIS λ_{max} (log ε): 221 (4.25), 275 (4.19), 282 (4.14). IR (cm^{-1}): 3432.67 (N(CH$_2$—)$_3$), 3028.66 (aromatic CH=), 2944.77 (het. CH$_2$—), 2869.56 (CH$_3$—), 2636.14, 2615.00, 2538.83, 1718.26, 1595.81, 1578.45, 1470.46, 1418.39, 1397.17, 1340.28, 1310.39, 1281.47, 1241.93 (O-CH aromatic), 1101.15, 1070.30, 1022.09, 945.91, 885.17, 742.46 (alif. CH$_2$—), 684.61. LC–MS: purity 99.50% t_R = 5.61, (ESI) m/z [M+H]$^+$ 310.28. Anal. calcd for $C_{18}H_{28}NOCl \times C_2H_2O_4$: C, 60.07; H, 7.56; N, 3.50. Found: C, 60.14; H, 7.76 N, 3.51.

4.1.15. 1-(6-(3-Chlorophenoxy)hexyl)homopiperidine hydrogen oxalate (16)

Synthesis from **5** (1.46 g, 0.005 mol) and homopiperidine (0.99 g, 0.01 mol), K_2CO_3 (2.07 g, 0.015 mol), KI (catalytic amount) in ethanol (105 mL) and water (20 mL). Obtained 0.7 g of oil. Purified by procedure A. Yield 45%. Raw product was transformed into oxalic acid salt yielding 0.74 g of final compound. Mp: 127–129 °C. $C_{18}H_{28}NOCl \times C_2H_2O_4$ (MW = 399.92). ^{1}H NMR (DMSO-d_6) δ: 7.29 (t, J = 8.7 Hz, 1H, Ph-5-H), 6.99–6.95 (m, 2H, Ph-2,4-H), 6.92–6.88 (m, 1H, Ph-6-H), 3.98 (t, J = 6.2 Hz, 2H, CH_2-O), 3.20–3.17 (m, 4H, hPip-2,6-CH_2), 3.04–2.99 (m, 2H, hPip-CH_2), 1.77–1.59 (m, 12H, hPip-3,4,5,6-CH_2, 2 × CH_2), 1.48–1.28 (m, 4H, 2 × CH_2). ^{13}C NMR (400 MHz, DMSO-d_6) δ: 165.24, 160.07, 134.18, 131.31, 120.81, 114.86, 114.02, 68.15, 56.67, 53.91, 40.61, 28.73, 26.53, 26.28, 25.45, 23.97, 23.42. UV–VIS λ_{max} (log ε): 221 (4.25), 229 (4.24), 275 (4.18), 282 (4.12). IR (cm^{-1}): 3437.49 (N(CH$_2$—)$_3$), 3030.59 (aromatic CH=), 2941.88 (het. CH$_2$—), 2860.87, 2709.50, 2648.75, 2536.90, 2362.37, 1701.87, 1635.34, 1596.77, 1470.46, 1398.14, 1310.39, 1249.65 (O-CH aromatic), 1155.15, 1073.19, 1034.62, 884.20, 721.25 (alif. CH$_2$—), 683.64. LC–MS: purity 100% t_R = 5.60, (ESI) m/z [M+H]$^+$ 310.28. Anal. calcd for $C_{18}H_{28}NOCl \times C_2H_2O_4$: C, 60.07; H, 7.56; N, 3.50. Found: C, 60.05; H, 7.69 N, 3.52.

4.1.16. 1-(6-(4-Chlorophenoxy)hexyl)piperidine hydrogen oxalate (17)

Synthesis from **6** (1.46 g, 0.005 mol) and piperidine (0.85 g, 0.01 mol), K_2CO_3 (2.07 g, 0.015 mol), KI (catalytic amount) in ethanol (105 mL) and water (20 mL). Obtained 0.25 g of oil. Purified by procedure B. Yield 17%. Raw product was transformed into oxalic acid salt yielding 0.22 g of final compound. Mp: 135–137 °C. $C_{17}H_{26}NOCl \times C_2H_2O_4$ (MW = 385.89). ^{1}H NMR (DMSO-d_6) δ: 7.31 (d, J = 9.2 Hz, 2H, Ph-3,5-H), 6.95 (d, J = 9.0 Hz, 2H, Ph-2,6-H), 3.94 (t, J = 6.3 Hz, 2H, CH_2-O), 3.36–3.26 (m, 4H, Pip-2,6-CH_2), 2.93 (t, J = 6.1 Hz, 2H, Pip-CH_2), 1.82–1.61 (m, 8H, 2 × CH_2, Pip-3,5-CH_2), 1.57–1.47 (m, 2H, Pip-4-H_2CH$_2$), 1.08–0.99 (m, 2H, CH_2), 0.97–0.80 (m, 2H, CH_2). ^{13}C NMR (400 MHz, DMSO-d_6) δ: 165.21, 157.95, 129.66, 124.50, 116.63, 68.11, 56.30, 52.38, 28.76, 26.33, 25.48, 23.57, 22.97, 21.99. UV–VIS λ_{max} (log ε): 209 (4.09), 215 (4.16), 225 (4.24), 282 (3.66), 398 (2.68). IR (cm^{-1}): 3428.38 (N(CH$_2$—)$_3$), 3020.52 (aromatic CH=), 2948.86 (het. CH$_2$—), 2868.54, 2690.77, 2538.19, 2362.37, 1703.63, 1656.40, 1595.56, 1471.54, 1394.95, 1332.21, 1244.27 (O-CH aromatic), 1169.39, 1069.24, 1055.30, 939.71, 836.56, 752.26 (alif. CH$_2$—), 669.35. LC–MS: purity 100% t_R = 5.35, (ESI) m/z [M+H]$^+$ 296.28. Anal. calcd for $C_{17}H_{26}NOCl \times C_2H_2O_4$: C, 59.14; H, 7.31; N, 3.63. Found: C, 59.08; H, 7.04 N, 3.64.

4.1.17. 1-(6-(4-Chlorophenoxy)hexyl)-3-methylpiperidine hydrogen oxalate (18)

Synthesis from **6** (1.46 g, 0.005 mol) and 3-methylpiperidine (0.99 g, 0.01 mol), K_2CO_3 (2.07 g, 0.015 mol), KI (catalytic amount) in ethanol (105 mL) and water (20 mL). Obtained 0.55 g of oil. Purified by procedure B. Yield 38%. Raw product was transformed

into oxalic acid salt yielding 0.37 g of final compound. Mp: 132–135 °C. $C_{18}H_{28}NOCl \times C_2H_2O_4$ (MW = 399.92). ^1H NMR (DMSO-d_6) δ: 7.30 (d, J = 9.0 Hz, 2H, Ph-3,5-*H*), 6.93 (d, J = 9.0 Hz, 2H, Ph-2,6-*H*), 3.93 (t, J = 6.3 Hz, 2H, C*H*$_2$-O), 3.37–3.27 (m, 2H, Pip-2,6-C*H*$_{2a}$), 2.93 (t, J = 6.1 Hz, 2H, Pip-C*H*$_2$), 2.73–2.66 (m, 1H, Pip-2-*H*$_e$), 2.51–2.57 (m, 1H, Pip-6-*H*$_e$), 1.75–1.50 (m, 8H, 2 × C*H*$_2$, Pip-4,5-C*H*), 1.47–1.30 (m, 4H, 2 × C*H*$_2$), 1.02 (def q, 1H, Pip-3-*H*), 0.86 (d, J = 6.7 Hz, 3H, C*H*$_3$). ^{13}C NMR (400 MHz, DMSO-d_6) δ: 165.29, 157.93, 129.66, 124.49, 116.63, 68.11, 57.84, 51.90, 30.50, 28.73, 26.30, 25.45, 23.57, 19.01. IR (cm^{-1}): 3420.79 (N(CH$_2$—)$_3$), 3030.02 (aromatic CH=), 2942.24 (het. CH$_2$—), 2871.79, 2871.79, 2729.70, 2686.52, 2539.54, 1722.85, 1597.58, 1491.53, 1392.88, 1284.25, 1247.05 (O-CH aromatic), 1168.28, 1090.58, 1013.03, 983.35, 830.93, 702.30 (alif. CH$_2$—), 666.87, 476.89. UV–VIS λ_{max} (log ε): 212 (4.20), 222 (4.26), 224 (4.26), 282 (3.78). LC–MS: purity 98% t_R = 5.59, (ESI) m/z [M+H]$^+$ 310.28. Anal. calcd for $C_{18}H_{28}NOCl \times C_2H_2O_4$: C, 60.07; H, 7.56; N, 3.50. Found: C, 59.94; H, 7.52 N, 3.46.

4.1.18. 1-(6-(4-Chlorophenoxy)hexyl)-4-methylpiperidine hydrogen oxalate (19)

Synthesis from **6** (1.46 g, 0.005 mol) and 4-methylpiperidine (0.99 g, 0.01 mol), K_2CO_3 (2.07 g, 0.015 mol), KI (catalytic amount) in ethanol (105 mL) and water (20 mL). Obtained 0.35 g of oil. Purified by procedure A followed by B. Yield 24%. Raw product was transformed into oxalic acid salt yielding 0.3 g of final compound. Mp: 129–131 °C. $C_{18}H_{28}NOCl \times C_2H_2O_4$ (MW = 399.92). ^1H NMR (DMSO-d_6) δ: 7.30 (d, J = 9.2 Hz, 2H, Ph-3,5-*H*), 6.93 (d, J = 9.0 Hz, 2H, Ph-2,6-*H*), 3.93 (t, J = 6.2 Hz, 2H, C*H*$_2$-O), 3.37–3.33 (m, 2H, Pip-2,6-C*H*$_{2a}$), 2.97–2.92 (m, 2H, Pip-C*H*$_2$), 2.86–2.78 (m, 2H, Pip-2,6-*H*$_e$), 1.77–1.59 (m, 7H, C*H*$_2$, Pip-3,5-C*H*$_2$, Pip-4-*H*), 1.47–1.30 (m, 6H, 4 × C*H*$_2$), 0.90 (d, J = 6.4 Hz, 3H, C*H*$_3$). IR (cm^{-1}): 3431.94 (N(CH$_2$—)$_3$), 3023.99 (aromatic CH=), 2940.34 (het. CH$_2$—), 2927.34, 2869.32, 2646.85, 2548.52, 1718.50, 1628.17, 1492.99, 1473.80, 1404.70, 1284.51, 1245.61 (O-CH aromatic), 1229.73, 1172.01, 1090.47, 1017.93, 945.17, 831.85, 700.23 (alif. CH$_2$—), 512.08. UV–VIS λ_{max} (log ε): 223 (4.25), 225 (4.24), 282 (3.76). LC–MS: purity 100% t_R = 5.69, (ESI) m/z [M+H]$^+$ 310.28. Anal. calcd for $C_{18}H_{28}NOCl \times C_2H_2O_4$: C, 60.07; H, 7.56; N, 3.50. Found: C, 59.93; H, 7.38; N, 3.52.

4.1.19. 1-(6-(4-Chlorophenoxy)hexyl)homopiperidine hydrogen oxalate (20)

Synthesis from **6** (1.46 g, 0.005 mol) and homopiperidine (0.99 g, 0.01 mol), K_2CO_3 (2.07 g, 0.015 mol), KI (catalytic amount) in ethanol (105 mL) and water (20 mL). Obtained 0.45 g of oil. Purified by procedure B. Yield 31%. Raw product was transformed into oxalic acid salt yielding 0.53 g of final compound. Mp: 127–129 °C. $C_{18}H_{28}NOCl \times C_2H_2O_4$ (MW = 399.92). ^1H NMR (DMSO-d_6) δ: 7.30 (d, J = 9.2 Hz, 2H, Ph-3,5-*H*), 6.93 (d, J = 9.0 Hz, 2H, Ph-2,6-*H*), 3.93 (t, J = 6.2 Hz, 2H, C*H*$_2$-O), 3.3–3.10 (m, 4H, hPip-2,6-C*H*$_2$), 3.02–2.97 (m, 2H, hPip-C*H*$_2$), 1.75–1.43 (m, 12H, hPip-3,4,5,6-C*H*$_2$, 2 × C*H*$_2$), 1.41–1.30 (m, 4H, 2 × C*H*$_2$). IR (cm^{-1}): 3428.37 (N(CH$_2$—)$_3$), 3016.69 (aromatic CH=), 2942.39 (het. CH$_2$—), 2863.90, 2638.12, 2535.47, 2361.48, 1717.47, 1697.76, 1598.54, 1494.04, 1452.26, 1405.09, 1341.13, 1289.48, 1250.90 (O-CH aromatic), 1089.58, 1027.49, 1006.54, 925.13, 828.78, 794.61, 705.29 (alif. CH$_2$—), 669.64, 474.55. UV–VIS λ_{max} (log ε): 226 (4.26), 282 (3.70). LC–MS: purity 100% t_R = 5.61, (ESI) m/z [M+H]$^+$ 310.35. Anal. calcd for $C_{18}H_{28}NOCl \times C_2H_2O_4$: C, 60.07; H, 7.56; N, 3.50. Found: C, 60.08; H, 7.07 N, 3.52.

4.1.20. 1-(7-(3-Chlorophenoxy)heptyl)piperidine hydrogen oxalate (21)

Synthesis from **7** (1.53 g, 0.005 mol) and piperidine (0.85 g, 0.01 mol), K_2CO_3 (2.07 g, 0.015 mol), KI (catalytic amount) in ethanol (105 mL) and water (20 mL). Obtained 0.56 g of oil. Purified by procedure A. Yield 55%. Raw product was transformed into oxalic acid salt yielding 0.63 g of final compound. Mp: 115–117 °C. $C_{18}H_{28}NOCl \times C_2H_2O_4$ (MW = 399.92). ^1H NMR (DMSO-d_6) δ: 7.27 (t, J = 8.7 Hz, 1H, Ph-5-*H*), 6.97–6.94 (m, 2H, Ph-2,4-*H*), 6.90–6.85 (m, 1H, Ph-6-*H*), 3.96 (t, J = 6.2 Hz, 2H, C*H*$_2$-O), 3.05 (br s, 4H, Pip-2,6-C*H*$_2$), 2.92 (t, J = 6.1 Hz, 2H, Pip-C*H*$_2$), 1.70–1.26 (br m, 16H, C*H*$_2$, Pip-3,4,5-C*H*$_2$, 5 × C*H*$_2$). ^{13}C NMR (400 MHz, DMSO-d_6) δ: 165.20, 160.09, 134.17, 131.29, 120.78, 114.85, 114.01, 68.24, 56.34, 52.37, 28.86, 28.65, 26.55, 25.66, 23.54, 22.96, 21.98. UV–VIS λ_{max} (log ε): 213 (4.28), 221 (4.28), 275 (4.20), 282 (4.15). IR (cm^{-1}): 3431.71 (N(CH$_2$—)$_3$), 3020.94 (aromatic CH=), 2938.98 (het. CH$_2$—), 2866.67, 2684.43, 2548.37, 1721.16, 1627.63, 1593.88, 1482.03, 1470.26, 1392.35, 1349.93, 1284.36, 1230.36 (O-CH aromatic), 1198.54, 1167.69, 1073.19, 1042.34, 1022.09, 868.77, 850.45, 775.24 (alif. CH$_2$—), 699.07, 680.75. LC–MS: purity 100% t_R = 5.75, (ESI) m/z [M+H]$^+$ 310.35. Anal. calcd for $C_{18}H_{28}NOCl \times C_2H_2O_4$: C, 60.07; H, 7.56; N, 3.50. Found: C, 59.91; H, 7.50; N, 3.59.

4.1.21. 1-(7-(3-Chlorophenoxy)heptyl)-3-methylpiperidine hydrogen oxalate (22)

Synthesis from **7** (1.53 g, 0.005 mol) and 3-methylpiperidine (0.99 g, 0.01 mol), K_2CO_3 (2.07 g, 0.015 mol), KI (catalytic amount) in ethanol (105 mL) and water (20 mL). Obtained 0.52 g of oil. Purified by procedure A. Yield 38%. Raw product was transformed into oxalic acid salt yielding 0.63 g of final compound. Mp: 112–115 °C. $C_{19}H_{30}NOCl \times C_2H_2O_4$ (MW = 413.93). ^1H NMR (DMSO-d_6) δ: 7.28 (t, J = 8.7 Hz, 1H, Ph-5-*H*), 6.97–6.94 (m, 2H, Ph-2,4-*H*), 6.90–6.85 (m, 1H, Ph-6-*H*), 3.96 (t, J = 6.3 Hz, 2H, C*H*$_2$-O), 3.38–3.21 (m, 2H, Pip-2,6-C*H*$_{2a}$), 2.93 (def t, 2H, Pip-C*H*$_2$), 2.68 (br s, 1H, Pip-2-*H*$_e$), 2.43–2.41 (m, 1H, Pip-6-*H*$_e$), 1.93 (br s, 2H, C*H*$_2$), 1.80–1.66 (m, 7H, Pip-3,4,5-C*H*, C*H*$_2$), 1.48–1.27 (m, 6H, 3 × C*H*$_2$), 0.86 (d, J = 6.7, 3H, C*H*$_3$). ^{13}C NMR (300 MHz, DMSO-d_6) δ: 165.20, 160.06, 134.15, 131.28, 120.77, 114.82, 113.99, 68.21, 57.83, 56.34, 51.81, 30.56, 28.83, 28.64, 26.54, 25.64, 23.56, 19.04. UV–VIS λ_{max} (log ε): 213 (4.25), 220 (4.28), 225 (4.28), 231 (4.26), 275 (4.19), 282 (4.14). IR (cm^{-1}): 3437.79 (N(CH$_2$—)$_3$), 2937.06 (aromatic CH=), 2852.34 (het. CH$_2$—), 2692.20 (CH$_3$—), 2502.19, 2413.48, 1801.19, 1771.30, 1712.48, 1594.84, 1467.56, 1455.99, 1394.28, 1282.43, 1248.68 (O-CH aromatic), 1092.48, 1024.98, 824.42, 755.96 (alif. CH$_2$—). LC–MS: purity 98.47% t_R = 6.06, (ESI) m/z [M+H]$^+$ 324.31. Anal. calcd for $C_{19}H_{30}NOCl \times C_2H_2O_4 \times 0.5\ H_2O$: C, 59.63; H, 7.86; N, 3.31. Found: C, 59.25; H, 8.20; N, 3.42.

4.1.22. 1-(7-(3-Chlorophenoxy)heptyl)-4-methylpiperidine hydrogen oxalate (23)

Synthesis from **7** (1.53 g, 0.005 mol) and 4-methylpiperidine (0.99 g, 0.01 mol), K_2CO_3 (2.07 g, 0.015 mol), KI (catalytic amount) in ethanol (105 mL) and water (20 mL). Obtained 0.65 g of oil. Purified by procedure A. Yield 58%. Raw product was transformed into oxalic acid salt yielding 0.4 g of final compound. Mp: 110–112 °C. $C_{19}H_{30}NOCl \times C_2H_2O_4$ (MW = 413.93). ^1H NMR (DMSO-d_6) δ: 7.28 (t, J = 8.7 Hz, 1H, Ph-5-*H*), 6.98–6.94 (m, 2H, Ph-2,4-*H*), 6.90–6.85 (m, 1H, Ph-6-*H*), 3.96 (t, J = 6.2 Hz, 2H, C*H*$_2$-O), 3.35–3.31 (m, 2H, Pip-2,6-C*H*$_{2a}$), 2.95–2.90 (m, 2H, Pip-C*H*$_2$), 2.80 (br s, 2H, Pip-2,6-*H*$_{2e}$), 1.75–1.48 (m, 7H, C*H*$_2$, Pip-3,5-C*H*$_2$, Pip-4-*H*), 1.44–1.30 (m, 8H, 4 × C*H*$_2$), 0.90 (d, J = 6.2 Hz, 3H, C*H*$_3$). ^{13}C NMR (400 MHz, DMSO-d_6) δ: 165.23, 160.10, 134.17, 131.29, 120.78, 114.85, 114.01, 68.24, 30.91, 28.86, 28.65, 28.47, 26.55, 25.66, 23.67, 21.30. UV–VIS λ_{max} (log ε): 207 (5.01), 219 (4.95), 276 (4.44), 283 (4.40), 399 (3.62), 563 (3.05). IR (cm^{-1}): 3421.10 (N(CH$_2$—)$_3$), 3066.26, 3028.66 (aromatic CH=), 2941.88 (het. CH$_2$—), 2870.52, 2857.99 (CH$_3$—), 2611.14, 2510.86, 1717.30, 1591.95, 1579.41, 1469.49, 1393.32, 1282.43, 1247.72 (O-CH aromatic), 1247.72, 1177.33, 1158.04, 1090.50, 1072.23, 1030.70, 944.95, 883.24,

766.57 (alif. CH_2—), 682.68. LC–MS: purity 100% t_R = 6.05, (ESI) m/z $[M+H]^+$ 324.31. Anal. calcd for $C_{19}H_{30}NOCl \times C_2H_2O_4$: C, 60.93; H, 7.79; N, 3.38. Found: C, 61.75; H, 8.35; N, 3.57.

4.1.23. 1-(7-(3-Chlorophenoxy)heptyl)homopiperidine hydrogen oxalate (24)

Synthesis from **7** (1.53 g, 0.005 mol) and homopiperidine (0.99 g, 0.01 mol), K_2CO_3 (2.07 g, 0.015 mol), KI (catalytic amount) in ethanol (105 mL) and water (20 mL). Obtained 0.72 g of oil. Purified by procedure B. Yield 62%. Raw product was transformed into oxalic acid salt yielding 0.7 g of final compound. Mp: 85–87 °C. $C_{19}H_{30}NOCl \times C_2H_2O_4$ (MW = 413.93). ^{1}H NMR (DMSO-d_6) δ: 7.29 (t, J = 8.7 Hz, 1H, Ph-5-*H*), 6.99–6.94 (m, 2H, Ph-2,4-*H*), 6.90–6.86 (m, 1H, Ph-6-*H*), 3.97 (t, J = 6.2 Hz, 2H, C*H*$_2$-O), 3.27–3.16 (m, 4H, hPip-2,7-C*H*$_2$), 3.00–2.97 (m, 2H, hPip-C*H*$_2$), 1.76–1.51 (m, 12H, 2 × C*H*$_2$, hPip-3,4,5,6-C*H*$_2$), 1.48–1.30 (m, 6H, 3 × C*H*$_2$). ^{13}C NMR (300 MHz, DMSO-d_6) δ: 165.30, 160.06, 134.14, 131.28, 120.76, 114.81, 113.99, 68.21, 56.66, 53.84, 28.83, 28.64, 26.54, 25.66, 23.95, 23.38. UV–VIS λ_{max} (log ε): 218 (4.29), 220 (4.29), 275 (4.20), 282 (4.14). IR (cm^{-1}): 3442.31 (N(CH_2—)$_3$), 3015.36 (aromatic CH=), 2938.98 (het. CH_2—), 2856.06, 2649.71, 1720.19, 1698.02, 1595.81, 1471.42, 1439.60, 1402.96, 1283.39 (O-CH aromatic), 1231.33, 1197.58, 1074.16, 1042.34, 855.28, 721.25 (alif. CH_2—), 704.85, 680.75. LC–MS: purity 98.59% t_R = 5.99, (ESI) m/z $[M+H]^+$ 324.31. Anal. calcd for $C_{19}H_{30}NOCl \times C_2H_2O_4$: C, 60.93; H, 7.79; N, 3.38. Found: C, 61.12; H, 7.91; N, 3.40.

4.1.24. 1-(7-(4-Chlorophenoxy)heptyl)piperidine hydrogen oxalate (25)

Synthesis from **8** (1.53 g, 0.005 mol) and piperidine (0.85 g, 0.01 mol), K_2CO_3 (2.07 g, 0.015 mol), KI (catalytic amount) in ethanol (105 mL) and water (20 mL). Obtained 0.5 g of oil. Purified by procedure A. Yield 48%. Raw product was transformed into oxalic acid salt yielding 0.55 g of final compound. Mp: 150–152 °C. $C_{18}H_{28}NOCl \times C_2H_2O_4$ (MW = 399.92). ^{1}H NMR (DMSO-d_6) δ: 7.29 (d, J = 9.2 Hz, 2H, Ph-3,5-*H*), 6.93 (d, J = 9.0 Hz, 2H, Ph-2,6-*H*), 3.93 (t, J = 6.3 Hz, 2H, C*H*$_2$-O), 3.29–3.05 (m, 4H, Pip-2,6-C*H*$_2$), 2.91 (t, J = 6.1 Hz, 2H, Pip-C*H*$_2$), 1.70–1.27 (br m, 16H, Pip-3,4,5-C*H*$_2$, 5 × C*H*$_2$). UV–VIS λ_{max} (log ε): 215 (4.27), 219 (4.29), 224 (4.30), 228 (4.30), 235 (4.27), 282 (4.15). IR (cm^{-1}): 3429.78 (N(CH_2—)$_3$), 3031.55 (aromatic CH=), 2940.91 (het. CH_2—), 2859.92, 2691.18, 2598.61, 2483.21, 1719.23, 1644.02, 1596.77, 1579.41, 1491.67, 1474.231, 1394.28, 1285.32, 1243.86 (O-CH aromatic), 1169.62, 1104.05, 1091.51, 1002.68, 961.43, 945.91, 823.46, 720.28 (alif. CH_2—), 667.25, 523.58. LC–MS: purity 100% t_R = 5.71, (ESI) m/z $[M+H]^+$ 310.28. Anal. calcd for $C_{18}H_{28}NOCl \times C_2H_2O_4$: C, 60.07; H, 7.56; N, 3.50. Found: C, 60.33; H, 8.01; N, 3.55.

4.1.25. 1-(7-(4-Chlorophenoxy)heptyl)-3-methylpiperidine hydrogen oxalate (26)

Synthesis from **8** (1.53 g, 0.005 mol) and 3-methylpiperidine (0.99 g, 0.01 mol), K_2CO_3 (2.07 g, 0.015 mol), KI (catalytic amount) in ethanol (105 mL) and water (20 mL). Obtained 0.73 g of oil. Purified by procedure A. Yield 45%. Raw product was transformed into oxalic acid salt yielding 0.65 g of final compound. Mp: 130–132 °C. $C_{19}H_{30}NOCl \times C_2H_2O_4$ (MW = 413.93). ^{1}H NMR (DMSO-d_6) δ: 7.30 (d, J = 9.2 Hz, 2H, Ph-3,5-*H*), 6.93 (d, J = 9.0 Hz, 2H, Ph-2,6-*H*), 3.93 (t, J = 6.3 Hz, 2H, C*H*$_2$-O), 3.35–3.25 (m, 2H, Pip-2,6-C*H*$_{2a}$), 2.92 (t, J = 6.1 Hz, 2H, Pip-C*H*$_2$), 2.67–2.63 (m, 1H, Pip-2-*H*$_e$), 2.47–2.41 (m, 1H, Pip-6-*H*$_e$), 1.89–1.27 (br m, 14H, Pip-4,5-C*H*$_2$, 5 × C*H*$_2$), 1.04 (def q, 1H, Pip-3-C*H*), 0.87 (d, J = 6.7 Hz, 3H, C*H*$_3$). ^{13}C NMR (300 MHz, DMSO-d_6) δ: 165.19, 157.94, 129.64, 124.44, 116.59, 68.16, 57.81, 51.84, 30.54, 28.88, 28.66, 26.53, 25.66, 23.55, 19.04. UV–VIS λ_{max} (log ε): 206 (3.81), 228 (4.08), 282 (3.37), 538 (2.14). IR (cm^{-1}): 3433.64 (N(CH_2—)$_3$), 2935.13 (aromatic CH=), 2857.99 (het. CH_2—), 2671.89, 2550.40 (CH_3—), 2361.41, 2342.12, 1718.26, 1701.87, 1625.70, 1597.73, 1492.63, 1473.35, 1402.96, 1280.50, 1245.79 (O-CH aromatic), 1168.65, 1092.48, 823.46, 721.25 (alif. CH_2—), 667.25. LC–MS: purity 100% t_R = 5.98, (ESI) m/z $[M+H]^+$ 324.31. Anal. calcd for $C_{19}H_{30}NOCl \times C_2H_2O_4$: C, 60.93; H, 7.79; N, 3.38. Found: C, 60.86; H, 8.10; N, 3.47.

4.1.26. 1-(7-(4-Chlorophenoxy)heptyl)-4-methylpiperidine hydrogen oxalate (27)

Synthesis from **8** (1.53 g, 0.005 mol) and 4-methylpiperidine (0.99 g, 0.01 mol), K_2CO_3 (2.07 g, 0.015 mol), KI (catalytic amount) in ethanol (105 mL) and water (20 mL). Obtained 0.75 g of oil. Purified by procedure A. Yield 46%. Raw product was transformed into oxalic acid salt yielding 0.78 g of final compound. Mp: 139–141 °C. $C_{19}H_{30}NOCl \times C_2H_2O_4$ (MW = 413.93). ^{1}H NMR (DMSO-d_6) δ: 7.30 (d, J = 9.2 Hz, 2H, Ph-3,5-*H*), 6.93 (d, J = 9.0 Hz, 2H, Ph-2,6-*H*), 3.93 (t, J = 6,3 Hz, 2H, C*H*$_2$-O), 3.35–3.31 (m, 2H, Pip-2,6-C*H*$_{2a}$), 2.95–2.89 (m, 2H, Pip-C*H*$_2$), 2.83–2.75 (m, 2H, Pip-2,6-*H*$_{2e}$), 1.76–1.48 (m, 7H, C*H*$_2$, Pip-3,5-C*H*$_2$, Pip-4-*H*), 1.44–1.31 (m, 8H, 4 × C*H*$_2$), 0.90 (d, J = 6.4 Hz, 3H, C*H*$_3$). ^{13}C NMR (300 MHz, DMSO-d_6) δ: 165.16, 157.93, 129.64, 124.44, 116.59, 68.16, 28.87, 28.64, 26.52, 25.67, 23.67. UV–VIS λ_{max} (log ε): 215 (4.26), 225 (4.30), 230 (4.29), 282 (4.23), 289 (4.19). IR (cm^{-1}): 3438.46 (N(CH_2—)$_3$), 3032.51 (aromatic CH=), 2930.31 (het. CH_2—), 2855.10 (CH_3—), 2713.35, 2570.65, 2553.29, 1719.23, 1638.23, 1596.77, 1491.67, 1474.31, 1391.39, 1281.47, 1242.90 (O-CH aromatic), 1170. 58, 1092.48, 1024.98, 823.46, 720.28 (alif. CH_2—), 655.32. LC–MS: purity 100% t_R = 6.05, (ESI) m/z $[M+H]^+$ 324.31. Anal. calcd for $C_{19}H_{30}NOCl \times C_2H_2O_4$: C, 60.93; H, 7.79; N, 3.38. Found: C, 60.91; H, 8.08; N, 3.50.

4.1.27. 1-(7-(4-Chlorophenoxy)heptyl)homopiperidine hydrogen oxalate (28)

Synthesis from **8** (1.53 g, 0.005 mol) and homopiperidine (0.99 g, 0.01 mol), K_2CO_3 (2.07 g, 0.015 mol), KI (catalytic amount) in ethanol (105 mL) and water (20 mL). Obtained 0.7 g of oil. Purified by procedure A. Yield 43%. Raw product was transformed into oxalic acid salt yielding 0.67 g of final compound. Mp: 128–131 °C. $C_{19}H_{30}NOCl \times C_2H_2O_4$ (MW = 413.93). ^{1}H NMR (DMSO-d_6) δ: 7.30 (d, J = 9.2 Hz, 2H, Ph-3,5-*H*), 6.93 (d, J = 9.0 Hz, 2H, Ph-2,6-*H*), 3.93 (t, J = 6.3 Hz, 2H, C*H*$_2$-O), 3.27–3.16 (m, 4H, hPip-2,7-C*H*$_2$), 3.02–2.98 (m, 2H, hPip-C*H*$_2$), 1.75–1.50 (m, 12H, 2 × C*H*$_2$, hPip-3,4,5,6-C*H*$_2$), 1.48–1.29 (m, 6H, 3 × C*H*$_2$). ^{13}C NMR (300 MHz, DMSO-d_6) δ: 165.26, 157.93, 129.64, 124.44, 116.59, 68.16, 56.66, 53.85, 28.86, 28.66, 26.53, 25.68, 23.96, 23.40. UV–VIS λ_{max} (log ε): 215 (4.26), 225 (4.30), 230 (4.30), 282 (4.23), 289 (4.19). IR (cm^{-1}): 3432.67 (N(CH_2—)$_3$), 3035.41 (aromatic CH=), 2937.06 (het. CH_2—), 2858.95, 2717.21, 2651.64, 2361.41, 1718.26, 1701.87, 1636.30, 1596.77, 1579.41, 1491.67, 1474.31, 1396.21, 1280.50, 1244.83 (O-CH aromatic), 1168.65, 955.56, 823.46, 721.24 (alif. CH_2—), 692.32, 666.29. LC–MS: purity 100% t_R = 5.96, (ESI) m/z $[M+H]^+$ 324.31. Anal. calcd for $C_{19}H_{30}NOCl \times C_2H_2O_4$: C, 60.93; H, 7.79; N, 3.38. Found: C, 61.08; H, 8.04; N, 3.46.

4.2. X-ray structure analysis

4.2.1. 1-(6-(4-Chlorophenoxy)hexyl)-4-methylpiperidine hydrogen oxalate (19)

Crystal data for **19**: $C_{18}H_{29}ClNO$, C_2HO_4, M = 399.90, monoclinic, space group $P2_1/c$, a = 8.2950(15) Å, b = 25.609(5) Å, c = 11.0624 (19) Å, β = 111.584(3) (°), V = 2185.2(7) Å^3, Z = 4, D_x = 1.216 g cm^{-3}, T = 296 K, μ = 0.203 mm^{-1}, λ = 0.71073 Å, data/parameters = 3731/253; final R_1 = 0.07.

The structures were solved by direct methods and refined with SHELXTL.[58] Crystallographic data (excluding structural factors) for the structure reported in this paper have been deposited at the Cambridge Crystallographic Data Centre and allocated with the deposition number CCDC 1022232.

4.3. Docking studies

In silico visualization of binding to histamine H_3R model obtained from GPCRM Modelling Server,[45] was held using Schrödinger MacroModel 9.7.[44] All of the tested compounds were used in their *N*-protonated form and generated using Schrödinger suite. For the tested set of compounds, energetically optimal conformers were found using ConfGen (MMFFs forcefield, PRCG, convergence threshold = 0.05, 20 steps per rotatable bond, max. ring conformations = 16). For all of the structures 5 energetically best conformations were used for docking.

Receptor grid was generated by GlideGrid module and validated with previously described *pitolisant* (Wakix®). Docking studies were performed via GlideDock module (OPLS 2001 force field, solvent = water, standard precision, post-docking minimization). Results were interpreted by the means of Docking Score functions. Receptor–ligand interactions were visualized using UCSF Chimera.[59,60]

4.4. Lipophilicity

Lipophilicity, by means of R_{M0} values, was estimated using RP-TLC planar method. Methanol/acetic acid/water (with constant, 10% acid concentration) solvent mixture was used as a mobile phase. Organic solvent concentration varied from 85% to 55%, by 5% for each step. Mobile phase compositions as well as concentrations were chosen experimentally. For each concentration, 10 μL of compounds methanol solution in 1 mg/mL concentration was used. Planar chromatographic chambers were saturated with proper mixture for 45 min. followed by 15 min. saturation together with the plate. Glass plates were then evaluated on the distance of 90 mm, dried and spots were visualized using iodide fumes. For each of the compounds, on the base of R_f values, R_M values were determined. R_{M0} values were read from R_M/methanol concentration charts, after extrapolation to zero methanol concentration.

4.5. Pharmacology

General remarks Competition binding data were analyzed by the software GraphPad Prism™ (200, version 3.02, San Diego, CA, USA), using non-linear least squares fit. Affinity values (K_i) were expressed as mean from at least two experiments in triplicates. K_i values were calculated from IC_{50} values according to Cheng–Prusoff equation.[61]

4.5.1. [^{3}H]N^α-methylhistamine hH_3R displacement assay

The displacement binding assay was carried out as described by Kottke et al.[35] In summary, frozen crude membrane preparations of HEK-293 cells stably expressing the full-length recombinant hH_3R were thawed, homogenized, incubated for 90 min at 25 °C and shook at 250 rpm with [^{3}H]N^α-methylhistamine (2 nM) and different concentrations of the test compounds (seven appropriate concentrations between 0.01 nM and 10 μM were used) in a final assay volume of 200 μl per well. Non-specific binding was determined in the presence of *pitolisant* (10 μM). In saturation binding experiments B_{max} was found to be 0.89 pmol/mg and the K_d value of [^{3}H]N^α-methylhistamine was 2.98 nM. The bound radioligand was separated from free radioligand by filtration through GF/B filters (pre-treated with 0.3% (m/v) polyethyleneimine) using an Inotech cell harvester (Dottikin, Switzerland). Unbound radioligand was removed by three washing steps with 0.3 mL/well of ice-cold 50 mM Tris–HCl buffer (pH 7.4) containing 120 mM NaCl. Scintillation cocktail was added and the liquid scintillation counting was performed with a Perkin Elmer Trilux Betacounter (Perkin Elmer, Germany).

4.5.2. cAMP accumulation assay in cells expressing hH_3R

Intracellular cAMP accumulation was measured with homogenous TR-FRET immunoassay, using LANCE *Ultra* cAMP kit (PerkinElmer) and HEK293 cells, stably expressing hH_3R. An antagonist dose–response experiments were performed in a total assay volume of 20 μL in white 384-well plates, using 300 cells/well. (*R*)(−)-α-Methylhistamine (15 nM), forskolin (10 μM) and antagonists in appropriate concentrations (in range 0.1 nM–10 μM) were added simultaneously to cell suspension. Cells stimulation was performed for 30 min at room temperature. After incubation period, five microliters of europium (Eu) chelate-labeled cAMP tracer and 5 μL of U*Light*-labeled anti-cAMP mAb working solutions were added, mixed and incubated for 1 h. TR-FRET signal was read on an EnSpire microplate reader (PerkinElmer). Measured TR-FRET signal was translated into actual quantities of produced cAMP on the basis of cAMP standard curve and obtained results were presented as % of maximal response. Sigmoidal dose–response curve fitting was performed with use of GraphPad Prism™ software (version 5.01, San Diego, CA, USA). Showed results represent the mean of three separate experiments, each performed in triplicates.

4.5.3. Anticonvulsant Screening Program

Anticonvulsant evaluation of compounds was performed and sponsored by National Institute of Neurological Disorders and Stroke, National Institutes of Health (Rockville, USA) for the Anticonvulsant Screening Program (ASP). Compounds were injected as suspensions in 0.5% methylcellulose at the selected doses (3, 10, 30, 100 or/and 300 mg/kg). As experimental animals male albino mice (CF-1 strain) and male albino rats (Sprague–Dawley) were used. Observations were carried out after 0.5 h and 4 h (sometimes additionally 0.25, 1 and 2 h) after administration. Groups of eight mice or four rats were employed. Phase 1 of ASP includes three tests performed in mice (ip): maximal electroshock (MES), subcutaneous pentylenetetrazole (scMET), and neurotoxicity (rotarod test). Compounds interested for ASP program, underwent additional tests including: MES and TOX tests in rats after po; MES and TOX tests in rats after ip; 6-Hz test in mice; quantitative MES, scMET and TOX in mice or/and rats ip; pilocarpine induced status epilepticus (rats, ip); corneal kindled mice model (ip); formalin test (mice, ip), and hippocampal slice culture neuroprotection assay in vitro.

4.5.3.1. Maximal electroshock seizure (MES) test. Seizures are elicited by 60 Hz alternating current (50 mA in mice and 150 mA in rats) delivered for 2 s by corneal electrodes. A drop of 0.5% tetracaine HCl in 0.9% NaCl solution was placed into each eye prior to applying electrodes. Protection is defined as abolition of the hindlimb tonic extension component of the seizure.[62,63]

4.5.3.2. Subcutaneous pentetrazole induced seizures (scMET). A dose of pentetrazole which induce convulsions in 97% of animals (CD97: 85 mg/kg mice or 56.4 mg/kg rats) was injected into a loose fold of skin in the midline of the neck. Animals were observed for 30 min for the presence or absence of a seizure. Failure of observing even a threshold seizure (a single episode of clonic spasm which remains at least 5 s) was classified as protection.[37]

4.5.3.3. Neurotoxicity (TOX) test. The rotarod test was used to evaluate neurotoxicity in rodents (mice, rats). was measured by. Animal was placed on a 1 inch diameter knurled plastic rod rotating at 6 rpm. The animal can maintain its equilibrium for long periods of time. Neurotoxicity was indicated if animal falls off this rotating rod three times during a 1-min period. In rats, neurological deficit was indicated by ataxia, loss of placing response and muscle tone.[64]

4.5.3.4. 6 Hz psychomotor seizure test. Compounds are preadministered to mice via ip injection. Corneal stimulation (0.2 ms monopolar rectangular pulses at 6 Hz and 32 mA for 3 s) was delivered by a constant-current device. Untreated animals display seizures after such stimulation described as minimal clonic phase, whereas mice not displaying this behavioral are considered protected.[65]

4.5.3.5. Pilocarpine induced status epilepticus (SE)[66]. Compounds were administered via ip to male Sprague Dawley rats (150–180 gm). Then pilocarpine (50 mg/kg; ip) is administered and treatment-effects were observed. In the initial convulsive-SE behavioral observation studies, adult rats received a dose of the investigated compound, which was found in (Quantitative Rat (ip) Study) to produce minimal motor impairment. Rats were dosed either immediately upon the first behavioral Stage 3 seizure (e.g., 0 min) or 30 min following the first behavioral Stage 3 seizure. The number of animals which protected from Stage 3 or greater Racine[67] scale seizures is determinated.

4.5.3.6. Corneal kindled mice model. Adult male CF1 mice were kindled to a criterion of 5 consecutive secondarily generalized seizures (stage 4 or 5, as described by Racine[67]) according to the corneal kindling protocol previously described.[39,68] Tested compound was administered to 4 fully kindled mice and tested at 0.5 h after dosing. Mice displaying a seizure score < 3 are considered protected.

4.5.3.7. Formalin test (mice, ip). The formalin test was performed according to the method of Tjolsen et al.[69] A sub-dermal injection of 0.5% formalin was made into the plantar region of the right hindpaw of a mouse. The response to the formalin injection is characterized by the mouse licking the affected paw. The investigational compounds or vehicle were administered ip at a dose 13 mg/kg (**20**) and 16 mg/kg (**26**). After 0.25 h formalin was sub-dermally injected into the plantar surface of the right hindpaw. Following the formalin injection, each animal was then observed for the first 2 min of each 5-min epoch until a total of 40 min has elapsed since the administration of the test compound or vehicle. The cumulative duration of licking (in seconds) during each 2-min recording period was measured for analysis across compound- and vehicle-pretreated groups.

4.5.3.8. In vitro hippocampal slice culture—neuroprotection assay. Test in vitro qualitative assessment of the ability of compound to prevent excitotoxic cell death. Organotypic hippocampal slice cultures, prepared as described by Stoppini et al.,[70] are treated with *N*-methyl-D-aspartate (NMDA) or kainic acid (KA) to induce neuronal death. Propidium iodide (PI), a membrane-impermeant compound is included in all wells of the culture plate. PI binds to the DNA of dead and dying cells and fluoresces. The intensity of the PI fluorescence is proportional to the amount of the cell death in the individual slices. Hippocampal slice cultures are treated with the excitotoxin alone, or with the excitotoxin and either one or two investigational compounds at the indicated concentrations. If neuroprotection occurs as a consequence of the added compound, slice cultures will have visibly reduced fluorescent intensity when compared to the slice cultures that have been treated with the excitotoxin alone.

4.5.4. Antiproliferative assay

4.5.4.1. Cell lines. Neuroblastoma IMR-32 cell line was provided by Department of Oncogenomics, Academisch Medisch Centrum, Amsterdam, Holland.[71,72] Human embryonic kidney HEK-293 cell line (ATCC CRL-1573) was kindly donated by Prof. Dr. Christa Müller (Pharmaceutical Institute, Pharmaceutical Chemistry I, University of Bonn).

4.5.4.2. Cell culture. HEK-293 and IMR-32 cell lines were cultured in Dulbecco's Modified Eagle's Medium—DMEM (Gibco) contained 10% fetal bovine serum (FBS), 100 mg·mL^{-1} streptomycin and 100 U·mL^{-1} penicillin. Cells were cultured in an atmosphere containing 5% of carbon dioxide at 37 °C.

4.5.4.3. In vitro antiproliferative assay. The cells were seeded in 96-well plates at a concentration of 2×10^4 cells/well (IMR-32) or 1.5×10^4 cells/well (HEK-293) in 200 μL culture medium. Next, the cell lines were cultured for 24 h to reach ~60% confluence. The stock solutions of examined H_3R ligands in DMSO were diluted into fresh growth medium. The maximal DMSO concentration did not exceed 1%. Next the H_3R ligands were added into the microtiter plates at the final concentrations 0.01–250 μM. After 48 h of incubation 20 μL of EZ4U labeling mixture (EZ4U Non-radioactive cell proliferation and cytotoxicity assay, Biomedica) was added to the each well according to the manufacturer protocol. The cells were next incubated for 5 h at 37 °C, 5% CO_2. The absorbance of the samples was measured using a PerkinElmer EnSpire microplate reader at 492 nm. GraphPad Prism 5.01 software was used to calculate the IC_{50} values. The activity of the standard drug Doxorubicin was estimated as we described previously.[73]

4.6. Physicochemical studies

4.6.1. In silico metabolism study

The computational procedure MetaSite 4.1.1[52] was used for prediction of H_3R ligands metabolic biotransformations in silico. MetaSite identifies the most likely sites of metabolism in examined compound and predicts the structures of the metabolites by considering two factors: thermodynamic factor (enzyme-substrate recognition) and kinetic factor describing the chemical transformations catalyzed by the enzymes.[74,75] The highest metabolism probability sites were analyzed during this study using either liver or cytochrome CYP3A4 model exclusively.

4.6.2. In vitro metabolism study

4.6.2.1. Reaction with recombinant human liver microsomes (HLMs). Commercial, pooled, human (adult male and female) liver microsomes (HLMs) from Sigma–Aldrich were used for all biotransformations. The reaction was carried out using 1 mg/mL HLMs in 200 μl of reaction buffer containing 0.1 M Tris–HCl (pH 7.4), NADPH Regeneration System (Promega) and histamine H_3R ligand with final volume of 50 μM. The reaction was initiated by adding 50 μL of Regeneration System after 5 min. of preincubation at 37 °C. The 200 μL of cold methanol was added to terminate the reaction after 2 h of incubation at 37 °C. The mixture was centrifuged at 13,000 rpm for 15 min. and next the LC/MS analysis of the supernatant was performed. Mass spectra were recorded on LC/MS system consisted of a Waters Acquity UPLC, coupled to a Waters TQD mass spectrometer (electrospray ionization mode ESI-tandem quadrupole).

4.6.2.2. CYP3A4 P450-Glo™ assay. The CYP3A4 P450-Glo™ assays (Promega) were performed according to the manufacturer's procedure. The enzymatic reactions were conducted in white polystyrene, flat-bottom Nunc™ MicroWell™ 96-Well Microplates (Thermo Scientific). The mixture consisting 0.5 pmol of CYP3A4 membranes and 4× Luciferin-PPXE in 100 mM Tris–HCl was titrated in 96-well plate. Next, an equal volume of the histamine H_3R ligand or Luciferin-Free Water was added to give one-half of the final reaction volume. After the 10-min pre-incubation

one-half of the final volume of 2× NADPH Regeneration System (*Promega*) was added to initiate CYP3A4 reaction. The reaction mixture was next stirred for 1 min and then incubated at 37 °C for 30 min. The final concentrations of H_3R ligands were in the range of 0.025–10 μM and the total volume of DMSO did not exceed of recommended by manufacturer 0.2%. The reaction mixture with inactive control membranes (control) was also prepared as described above. Afterwards, to initiate the luminescence the reconstituted Luciferin Detection Reagent containing firefly luciferase was added. The luminescence was measured with a PerkinElmer EnSpire microplate reader in luminescence mode after 20 min incubation of the reaction mixture at room temperature. For calculation the total luminescence, the average luminescence of the control reaction containing inactive membranes was subtracted from the luminescence of CYP3A4 containing reactions. The luminescence of the reactions containing Luciferin-Free Water instead of the tested compound indicated the total (100%) CYP3A4 activity.[74] The IC_{50} value of the reference compound ketoconazole was determined and calculated as we described previously.[75]

Acknowledgements

We would like to thank prof James P. Sables, prof. Jeff Jiang and Tracy Chen, Ph.D. for providing the results of anticonvulsant assays through ASP at National Institute of Neurological Disorders and Stroke, National Institutes of Health (Rockville, USA). We grateful thank Senior scientist Mohamed Hamdi from Department of Oncogenomics Academisch Medisch Centrum Amsterdam, Holland for providing neuroblastoma IMR-32 cell line. We sincerely acknowledge Nicolas Levoin from Bioprojet Biotech for providing the histamine H_3R homology model, and Bioprojet for providing HEK H_3R cell lines. The authors are grateful to Maria Kaleta (Krakow, Poland) for excellent technical assistance in chemical synthesis part of the project and to Tim Kottke and Lilia Weizel (Frankfurt, Germany) and Agnieszka Olejarz (Krakow, Poland) for excellent support in pharmacological screening and to Natalia Groth (Krakow, Poland) for technical assistance in ADME-Tox screening. The authors acknowledge the partial support of National Science Center granted on the basis of decision Nos. DEC-2011/02/A/NZ4/00031 and K/ZDS/004689, of the European GLISTEN—CM1207 as well as of the DFG INST 208/664-1 FUGG.

Supplementary data

Supplementary data associated with this article can be found, in the online version, at http://dx.doi.org/10.1016/j.bmc.2015.11.021. These data include MOL files and InChiKeys of the most important compounds described in this article.

References and notes

1. Parsons, M. E.; Gannelin, C. R. *Br. J. Pharmacol.* **2006**, *147*, S127.
2. Tiligada, E.; Kyriakidis, K.; Chazot, P. L.; Passani, M. B. *CNS Neurosci. Ther.* **2011**, *17*, 620.
3. Walter, M.; Stark, H. *Front. Biosci. (Schol. Ed.)* **2012**, *4*, 461.
4. Schlicker, E.; Kathmann, N. In *The Histamine H3 Receptor*; Leurs, R., Timmerman, H., Eds.; A Target for New Drugs; Elsevier Science B.V., 1998; pp 13–26.
5. Blandina, P.; Bacciottini, L.; Giovannini, M. G.; Mannaioni, P. F. In *The Histamine H3 Receptor*; Leurs, R., Timmerman, H., Eds.; A Target for New Drugs; Elsevier Science B.V., 1998; pp 27–40.
6. Tiligada, E.; Zampeli, E.; Sander, K.; Stark, H. *Expert Opin. Invest. Drugs* **2009**, *18*, 1519.
7. Vohora, D.; Bhowmik, M. *Front. Syst. Neurosci.* **2012**, *6*, 72.
8. Łażewska, D.; Kieć-Kononowicz, K. *Expert Opin. Ther. Patents* **2014**, *24*, 89.
9. Incerti, M.; Flammini, L.; Saccani, F.; Morini, G.; Comini, M.; Coruzzi, M.; Barocelli, E.; Ballabeni, V.; Bertoni, S. *ChemMedChem* **2010**, *5*, 1143.
10. Darras, F. H.; Pockes, S.; Huang, G.; Wehle, S.; Strasser, A.; Wittmann, H.-J.; Nimczick, M.; Sotriffer, A. C.; Decker, M. *ACS Chem. Neurosci.* **2014**, *5*, 225.
11. Nikolic, K.; Filipoc, S.; Agbaba, D.; Stark, H. *CNS Neurosci. Ther.* **2014**, *20*, 613.
12. Apelt, J.; Ligneau, X.; Pertz, H. H.; Arrang, J. M.; Ganellin, C. R.; Schwartz, J. C.; Schunack, W.; Stark, H. *J. Med. Chem.* **2002**, *45*, 1128.
13. Bhowmik, M.; Khanam, R.; Vohora, D. *Br. J. Pharmacol.* **2012**, *167*, 1398.
14. Fisher, R. S.; Acevedo, C.; Arzimanoglou, A.; Bogacz, A.; Cross, J. H.; Elger, C. E.; Engel, J., Jr; Forsgren, L.; French, J. A.; Glynn, M.; Hesdorffer, D. C.; Lee, B. I.; Mathern, G. W.; Moshé, S. L.; Perucca, E.; Scheffer, I. E.; Tomson, T.; Watanabe, M.; Wiebe, S. *Epilepsia* **2014**, *55*, 475.
15. Lason, W.; Chlebicka, M.; Rejdak, K. *Pharmacol. Rep.* **2013**, *65*, 787.
16. Kamei, C. *Behav. Brain Res.* **2001**, *124*, 243.
17. Ago, J.; Ishikawa, T.; Matsumoto, N.; Ashequr Rahman, M.; Kamei, C. *Epilepsy Res.* **2006**, *72*, 1.
18. Miyata, I.; Saegusa, H.; Sakurai, M. *Pediatr. Int.* **2011**, *53*, 706.
19. Singh, E.; Pillai, K. K.; Mehndiratta, M. *Basic Clin. Pharmacol. Toxicol.* **2014**, *115*, 373.
20. Sadek, B.; Shehab, S.; Więcek, M.; Subramanian, D.; Shafiullah, M.; Kieć-Kononowicz, K.; Adem, A. *Bioorg. Med. Chem. Lett.* **2013**, *23*, 4886.
21. Sadek, B.; Schwed, J. S.; Subramanian, D.; Weizel, L.; Walter, M.; Adem, A.; Stark, H. *Eur. J. Med. Chem.* **2014**, *77*, 269.
22. Bhowmik, M.; Saini, N.; Vohora, D. *Brain Res.* **2014**, *1581*, 129.
23. Bitner, R. S.; Markosyan, S.; Nikkel, A. L.; Brioni, J. D. *Neuropharmacology* **2011**, *60*, 460.
24. Schwartz, J. C. *Br. J. Pharmacol.* **2011**, *163*, 713.
25. Kuhne, S.; Wijtmans, M.; Lim, H. D.; Leurs, R.; de Esch, I. J. P. *Expert Opin. Invest. Drugs* **2011**, *20*, 1629.
26. Schwartz, J.-C. 43rd Annual EHRS Meeting, Lyon, France, 2014, May 7–10, Book of Abstracts, p 20.
27. Kasteleijn-Nolst Trenité, D.; Parain, D.; Genton, P.; Masnou, P.; Schwartz, J. C.; Hirsch, E. *Epilepsy Behav.* **2013**, *28*, 66.
28. Łażewska, D.; Ligneau, X.; Schwartz, J.-C.; Schunack, W.; Stark, H.; Kieć-Kononowicz, K. *Bioorg. Med. Chem.* **2006**, *14*, 3522.
29. Łażewska, D.; Kuder, K.; Ligneau, X.; Schwartz, J. C.; Schunack, W.; Stark, H.; Kieć-Kononowicz, K. *Bioorg. Med. Chem.* **2008**, *16*, 8729.
30. Łażewska, D.; Kuder, K.; Ligneau, X.; Camelin, J.-C.; Schunack, W.; Stark, H.; Kieć-Kononowicz, K. *Bioorg. Med. Chem.* **2009**, *17*, 3037.
31. Bajda, M.; Kuder, K. J.; Łażewska, D.; Kieć-Kononowicz, K.; Więckowska, A.; Ignasik, M.; Guzior, N.; Jończyk, J.; Malawska, B. *Arch. Pharm. Chem. Life Sci.* **2012**, *345*, 591.
32. Sadek, B.; Kuder, K.; Subramanian, D.; Shafiullah, M.; Stark, H.; Łażewska, D.; Adem, A.; Kieć-Kononowicz, K. *Behav. Pharmacol.* **2014**, *25*, 245.
33. Beasley, Y. M.; Petrow, V.; Stephenson, O. *J. Pharm. Pharmacol.* **1958**, *10*, 47.
34. Marquet, J.; Cayon, E.; Martin, X.; Casado, F.; Gallardo, I.; Moreno, M.; Lluch, J. M. *J. Org. Chem.* **1995**, *60*, 3814.
35. Kottke, T.; Sander, K.; Weizel, L.; Schneider, E. H.; Seifert, R.; Stark, H. *Eur. J. Pharmacol.* **2011**, *654*, 200.
36. Stables, J. P.; Kupferberg, H. J. In *Molecular and Cellular Targets for Antiepileptic Drugs*; Avanzin, G., Regesta, P., Tanganelli, A., Avoli, M., Eds.; John Libbey&Company Ltd: London, 1997; Vol. 23129, pp 191–198.
37. White, S. H.; Woodhead, J. H.; Wilcox, K. S.; Kupferberg, H. J.; Wolf, H. H. In *Antiepileptic Drugs*; Levy, R. H., Mattson, R. H., Meldurm, B. S., Perucca, E., Eds., 5th ed.; Lippincott Williams&Wilkins: Philadelphia, 2002; pp 36–48.
38. Loscher, W. *Seizure* **2011**, *20*, 359.
39. Rowley, N. M.; White, H. S. *Epilepsy Res.* **2010**, *92*, 163.
40. Dingledine, R.; Varvel, N. H.; Dudek, F. E. *Adv. Exp. Med. Biol.* **2014**, *813*, 109.
41. Waszkielewicz, A. M.; Gunia, A.; Słoczyńska, K.; Marona, H. *Curr. Med. Chem.* **2011**, *18*, 4344.
42. Barrot, M. *Neuroscience* **2012**, *211*, 39.
43. Strasser, A.; Wittmann, H. J.; Buschauer, A.; Schneider, E. H.; Seifert, R. *Trends Pharmacol. Sci.* **2013**, *34*, 13.
44. (a) Friesner, R. A.; Murphy, R. B.; Repasky, M. P.; Frye, L. L.; Greenwood, J. R.; Halgren, T. A.; Sanschagrin, P. C.; Mainz, D. T. *J. Med. Chem.* **2006**, *49*, 6177–6196; (b) Halgren, T. A.; Murphy, R. B.; Friesner, R. A.; Beard, H. S.; Frye, L. L.; Pollard, W. T.; Banks, J. L. *J. Med. Chem.* **2004**, *47*, 1750–1759; (c) Friesner, R. A.; Banks, J. L.; Murphy, R. B.; Halgren, T. A.; Klicic, J. J.; Mainz, D. T.; Repasky, M. P.; Knoll, E. H.; Shaw, D. E.; Shelley, M.; Perry, J. K.; Francis, P.; Shenkin, P. S. *J. Med. Chem.* **2004**, *47*, 1739–1749; Small-Molecule Drug Discovery Suite 2014–4: Glide, version 6.5, Schrödinger, LLC, New York, NY, 2014.
45. Levoin, N.; Calmels, T.; Poupardin-Olivier, O.; Labeeuw, O.; Danvy, D.; Robert, P.; Berrebi-Bertrand, I.; Ganellin, C. R.; Schunack, W.; Stark, H.; Capet, M. *Arch. Pharm. Chem. Life Sci.* **2008**, *341*, 610.
46. Schlegel, B.; Laggner, C.; Meier, R.; Langer, T.; Schnell, D.; Seifert, R.; Stark, H.; Hoeltje, H. D.; Sippl, W. *J. Comput. Aided Mol. Des.* **2007**, *21*, 437.
47. Sherma, J. *Anal. Chem.* **2002**, *74*, 2653.
48. CS Chem Office, Version ultra 8.0.3, Cambridge Soft Corporation, Software Publishers Association, Washington D.C., 20036, 452–1600.
49. Marvin was used for drawing, displaying and characterizing chemical structures, substructures and reactions, Marvin. 14.8.25.0, 2014, ChemAxon (http://www.chemaxon.com). Calculator Plugins were used for structure property prediction and calculation, Marvin 14.8.25.0, 2014.
50. Kerns, E. H.; Di, L. *Drug-like Properties: Concepts, Structure Design and Methods*; Academic Press: Burlington, MA, 2008.
51. Cruciani, G.; Carosati, E.; De Boeck, B.; Ethirajulu, K.; Mackie, C.; Howe, T.; Vianello, R. *J. Med. Chem.* **2005**, *48*, 6970.
52. (a) Cruciani, G.; Valeri, A.; Goracci, L.; Pellegrino, R. M.; Buonerba, F.; Baroni, M. *J. Med. Chem.* **2014**, *57*, 6183–6196; (b) Zhou, D.; Afzelius, L.; Grimm, S. W.; Andersson, T. B.; Zauhar, R. J.; Zamora, I. *Drug Metab. Dispos.* **2006**, *34*, 976–983; (c) Ahlström, M. M.; Ridderström, M.; Zamora, I.; Luthman, K. *J Med Chem.*

2007, *50*, 4444–4452; Metasite, version 4.1.1; Molecular Discovery Ltd., Pinner, Middlesex, UK, 2013.
53. Meier, G.; Apelt, J.; Reichert, U.; Grassmann, S.; Ligneau, X.; Elz, S.; Leurquin, F.; Ganellin, C. R.; Schwartz, J.-C.; Schunack, W.; Stark, H. *Eur. J. Pharm. Sci.* **2001**, *13*, 249.
54. Carbonara, G.; Fracchiolla, G.; Loiodice, F.; Tortorella, P.; Conte-Caerino, D.; de Luca, A.; Liantonio, A. *Il Farmaco* **2001**, *56*, 749.
55. Khalafi-Nezhad, A.; Soltani Rad, M. N.; Mohabatkar, H.; Asrari, Z.; Hemmateenejada, B. *Bioorg. Med. Chem.* **2005**, *13*, 1931.
56. Wang, L.; Yang, W.; Wang, K.; Zhu, J.; Shen, F.; Hu, Y. *Bioorg. Med. Chem. Lett.* **2012**, *22*, 4887.
57. Hickey, D. M. B.; Ife, R. J.; Leach, C. A.; Pinto, I. L.; Porter, R. A.; Smith, S.A. WO99/24420, 1999.
58. Sheldrick, G. M. *Acta Crystallogr., Sect. A* **2008**, *64*, 112.
59. Molecular graphics and analyses were performed with the UCSF Chimera package. Chimera is developed by the Resource for Biocomputing, Visualization, and Informatics at the University of California, San Francisco (supported by NIGMS P41-GM103311); UCSF Chimera–a visualization system for exploratory research and analysis.
60. Pettersen, E. F.; Goddard, T. D.; Huang, C. C.; Couch, G. S.; Greenblatt, D. M.; Meng, E. C.; Ferrin, T. E. *J. Comput. Chem.* **2004**, *25*, 1605.
61. Cheng, Y.; Prusoff, W. H. *Biochem. Pharmacol.* **1973**, *22*, 3099.
62. Swinyard, E. A.; Woodhead, J. H.; White, H. S.; Franklin, M. R. General Principles: Experimental Selection, Quantification, and Evaluation of Anticonvulsants. In *Antiepileptic Drugs*; Levy, R. H., Mattson, R. H., Melrum, B., Penry, J. K., Dreifuss, F. E., Eds., 3rd ed.; Raven Press: New York, 1989; pp 85–102.
63. White, H. S.; Woodhead, J. H.; Franklin, M. R. General Principles: Experimental Selection, Quantification, and Evaluation of Antiepileptic Drugs. In *Antiepileptic Drugs*; Levy, R. H., Mattson, R. H., Meldrum, B., Eds., 4th ed.; Raven Press: New York, 1995; pp 99–110.
64. Dunham, M. S.; Miya, T. A. *J. Am. Pharm. Assoc. Sci. Ed.* **1957**, *46*, 208.
65. Barton, M. E.; Klein, B. D.; Wolf, H. H.; White, H. S. *Epilepsy Res.* **2001**, *47*, 217.
66. Lehmkuhle, M. J.; Thomson, K. E.; Scheerlinck, P.; Pouliot, W.; Greger, B.; Dudek, F. E. *J. Neurophysiol.* **2009**, *101*, 1660.
67. Racine, R. J. *Electroencephalogr. Clin. Neurophysiol.* **1972**, *32*, 281.
68. Matagne, A.; Klitgaard, H. *Epilepsy Res.* **1998**, *31*, 59.
69. Tjølsen, A.; Berge, O. G.; Hunskaar, S.; Rosland, J. H.; Hole, K. *Pain* **1992**, *51*, 5.
70. Stoppini, L.; Buchs, P.-A.; Muller, D. *J. Neurosci. Methods* **1991**, *37*, 173.
71. Cheng, N. C.; Van Roy, N.; Chan, A.; Beitsma, M.; Westerveld, A.; Speleman, F.; Versteeg, R. *Oncogene* **1995**, *10*, 291.
72. Tumilowicz, J. J.; Nichols, W. W.; Cholon, J. J.; Greene, A. E. *Cancer Res.* **1970**, *30*, 2110.
73. Grosicki, M.; Latacz, G.; Szopa, A.; Cukier, A.; Kieć-Kononowicz, K. *Acta Biochim. Pol.* **2014**, *61*, 29.
74. Cali, J. J.; Ma, D.; Sobol, M.; Simpson, D. J.; Frackman, S.; Good, T. D.; Daily, W. J.; Liu, D. *Expert Opin. Drug Metab. Toxicol.* **2006**, *2*, 629.
75. Łażewska, D.; Więcek, M.; Ner, J.; Kamińska, K.; Kottke, T.; Schwed, J. S.; Zygmunt, M.; Karcz, T.; Olejarz, A.; Kuder, K.; Latacz, G.; Grosicki, M.; Sapa, J.; Karolak-Wojciechowska, J.; Stark, H.; Kieć-Kononowicz, K. *Eur. J. Med. Chem.* **2014**, *83*, 534.